Overload Behavior of Pretensioned Prestressed Concrete I-Beams With Web Reinforcement

JOHN M. HANSON and C. L. HULSBOS
Respectively, Research Instructor of Civil Engineering and Research Professor of Civil Engineering, Lehigh University

The results of ultimate static strength tests on 18 pretensioned prestressed concrete I-beams with web reinforcement are presented. The principal variables in the test program were the shear-span-to-effective-depth ratio, which varied between 2.54 and 6.34, and the percentage of web reinforcement. The beams had an overall depth of 18 in. and the majority of the tests were conducted on a shear-span-to-effective-depth ratio of 3.39, for which the web reinforcement percentage was varied from 0 to 1.22. The behavior of the test beams under overloads to failure is discussed in detail. Requirements for the amount of web reinforcement based on the current AASHO specifications are compared with the test results. In addition, procedures for improved design of the web reinforcement are considered.

•AN ULTIMATE strength design of a concrete structure must be based generally on the following five factors: static strength, fatigue strength, stability, deflection, and durability. To be satisfactory, a structure must have the desired degree of safety with respect to each of these factors. For prestressed concrete bridge beams, stability, deflection, and durability are generally factors of lesser importance. The ultimate static strength is usually the factor of paramount importance. However, where many repeated loads of large magnitude can be expected, the fatigue strength of the member may be of equal importance.

This investigation (1) was undertaken to study the ultimate static strength of prestressed concrete I-beams with web reinforcement. The results of 18 tests on simply supported beams subjected to a symmetrical two-point loading, designated as the E Series and given in Table 1, are presented in this report. Sixteen of these tests were single-cycle static load tests; that is, the load was increased in increments, without unloading, until the ultimate capacity of the member was reached. The remaining two tests were repeated load tests. Only data taken from the first load cycle of the repeated load tests are included herein.

The principal variables in the test program were the shear-span-to-effective-depth ratio, which ranged between 2.54 and 6.34, and the percentage of web reinforcement. Concrete strength and prestressing were held as nearly constant as possible. Most of the tests, however, were conducted on a shear-span-to-effective-depth ratio of 3.39, for which the web reinforcement percentage ranged from 0 to 1.22. Corresponding to this particular shear span, No. 3 stirrups with a yield point of 55,500 psi, and the average concrete strength of 7,000 psi, the percentage of web reinforcement required by Paragraph 1.13.13 of the Standard Specifications for Highway Bridges (AASHO) is 0.85.

Paper sponsored by Committee on Bridges.

TABLE 1

OUTLINE OF TESTS

Shear Span, a (ft)	Web Reinforcement			Beam Designation
	Size (no.)	Spacing (in.)	Percent	
3	2D	8.75	0.374	E.14
	2D	8.75	0.374	E.15
4	-	-	0	E.4
	3D	6	1.22	E.5
	3D	8	0.917	E.6
	3D	10	0.733	E.7
	3S	6	0.611	E.8
	3S	8	0.458	E.9
	3S	6	0.611	E.10F[a]
	3S	8	0.458	E.11F[a]
	3S	10	0.367	E.12
	2D	8.75	0.374	E.13
	2S	6	0.272	E.16
	2S	8	0.204	E.17
	2S	10	0.163	E.18
5	-	-	0	E.3
6	-	-	0	E.2
7.5	-	-	0	E.1

[a] F indicates two repeated load tests.

NOTATION

a = length of shear span;
A = area of beam cross-section;
A_v = area of vertical stirrup;
b = width of compression flange;
b' = width of web;
d = distance from concrete top fibers to centroid of strand;
e = eccentricity of c.g.s. with respect to c.g.;
E_c = modulus of elasticity of the concrete;
f_c' = ultimate compressive strength of concrete at test;
f_{ci}' = ultimate compressive strength of concrete at prestress release;
f_r' = modulus of rupture strength of concrete at test;
f_t' = flexural tensile strength of concrete at test;
f_u' = ultimate tensile strength of stirrups;
f_y' = yield point of stirrups;
F = prestress force at test;
F_i = initial prestress force, before prestress release;
ℓ_e = distance from junction of web and top flange to lowest level at which stirrups may be regarded as effective;
M_d = dead load moment;
M_u = static ultimate moment;
M_c^f = flexural cracking moment;

Q = moment about the c.g. of the area on one side of horizontal section on which shearing stress is desired;
r = percentage of web reinforcement, $100\ A_v/b's$;
s = spacing of vertical stirrups;
V_c = shear carried by concrete;
V_d = dead load shear;
V_w = shear carried by stirrups;
V_u = ultimate shear;
V_c^f = shear causing flexural cracking;
V_c^{dt} = shear causing diagonal tension cracking;
V_c^{fs} = shear causing flexure shear cracking;
V_u^f = shear causing flexural failure;
Z = section modulus;
β = dimensionless factor which, when multiplied by d, determines effective horizontal projection of inclined crack;
θ = angle, with respect to horizontal, of compressive stress trajectory;
σ = normal stress;
σ_t = principal tensile stress;
σ_t^{cg} = principal tensile stress at c.g. of beam cross-section; and
τ = shearing stress.

TEST SPECIMENS

Description

A doubly symmetric I-shaped cross-section with a total-depth-to-flange-width ratio of 2 and a flange-to-web-width ratio of 3 was used for all 18 beam specimens. Each beam was 17 ft 6 in. in length, providing a test span of 15 ft and an overhang at each reaction of 1 ft 3 in. Details of the test beams are shown in Figure 1.

Size, spacing, and percentage of web reinforcement are given in the outline of tests in Table 1. Except for E.13 and E.14, each stirrup consisted of either one or two U-shaped bars, referred to as S or D. Where only one bar was used, each successive bar was placed so that the U opened to the opposite side of the test beam. In E.13 and E.14 inverted L-shaped bars were used, and each stirrup consisted of two bars.

Six 7/16-in. diameter strands were used as the prestressing elements in each beam. All strands were straight, and each strand was pretensioned to a nominal initial force of 18.9 kips, providing a total initial design prestress force of 113.4 kips. Assuming losses of 8 percent in the prestress force at transfer, the initial stresses in the top and bottom concrete fibers, based on the transformed section and neglecting dead weight, are 210-psi tension and 2,150-psi compression, respectively.

Materials

Ready-mixed concrete was used in casting the test beams, having a cement-to-sand-to-coarse-aggregate ratio of approximately 1:1.8:2.3. The mix contained 7.5 sk/cu yd of Type III portland cement. The maximum size of the coarse aggregate was $\frac{3}{4}$ in. Gradation of the aggregate conformed to Pennsylvania Department of Highways specifications. Mixes were made in either 2 or 2.5 cu yd batches, sufficient to cast three test beams at one time. Slump varied between $1\frac{1}{2}$ and $2\frac{3}{4}$ in., and concrete strength at the time of test of all beams was approximately 7,000 psi.

The prestressing strand was a $\frac{7}{16}$-in. diameter, seven wire, uncoated, stress-relieved, high tensile strength strand. A stress-strain curve for the strand, determined from a tension test conducted in the laboratory, is shown in Figure 2. Failure occurred in the testing machine grips at an ultimate load of 26.3 kips. The stress-strain curve in Figure 2 was virtually identical with the stress-strain curve provided by the manufacturer, which indicated that the strand had an ultimate load of 27.5 kips, corresponding

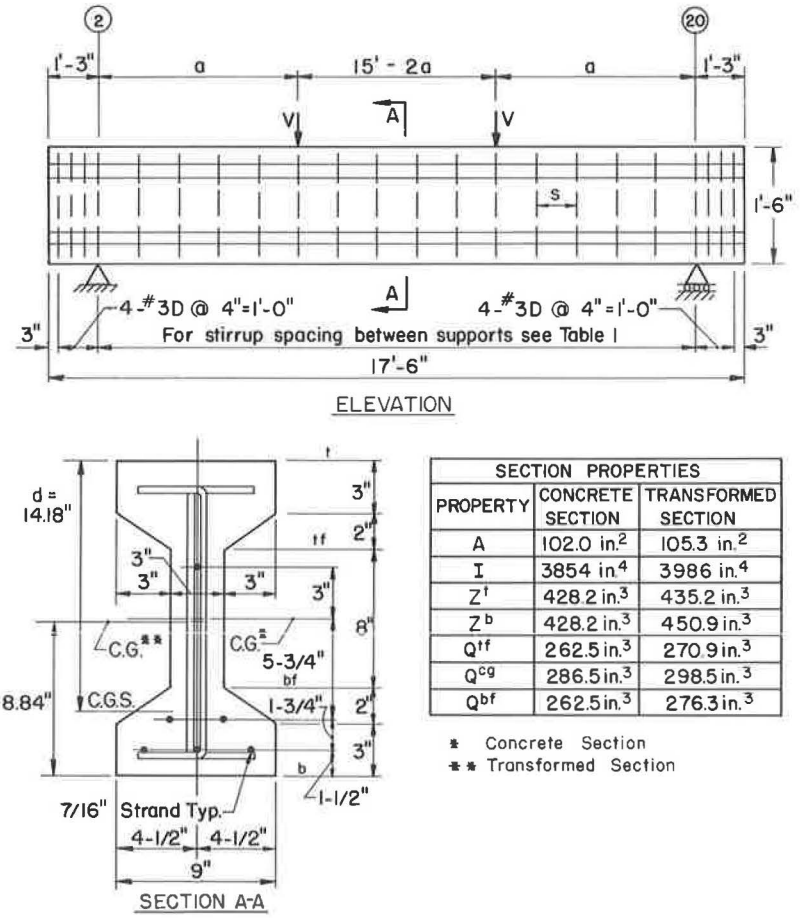

SECTION PROPERTIES		
PROPERTY	CONCRETE SECTION	TRANSFORMED SECTION
A	102.0 $in.^2$	105.3 $in.^2$
I	3854 $in.^4$	3986 $in.^4$
Z^t	428.2 $in.^3$	435.2 $in.^3$
Z^b	428.2 $in.^3$	450.9 $in.^3$
Q^{tf}	262.5 $in.^3$	270.9 $in.^3$
Q^{cg}	286.5 $in.^3$	298.5 $in.^3$
Q^{bf}	262.5 $in.^3$	276.3 $in.^3$

* Concrete Section
** Transformed Section

Figure 1. Details of test beams.

to an ultimate stress equal to 252.5 ksi, and 5.1 percent elongation in 24 in. The surface of the strand was free from rust, and care was taken to avoid getting any grease on the strand during the fabrication operation.

The web reinforcement was fabricated from hot rolled No. 2 or No. 3 deformed bars. For the No. 2 bar, the yield point stress, f'_y, was 59,500 psi and the ultimate stress, f'_u, was 85,700 psi, based on an area of 0.049 sq in. For the No. 3 bar, f'_y was 55,500 psi and f'_u was 82,700 psi, based on an area of 0.11 sq in. The values of f'_y and f'_u for the No. 2 and No. 3 bars are an average of 12 and 3 tension tests, respectively.

Fabrication

The test beams were fabricated in a prestressing bed set up in the laboratory. The length of the bed was sufficient to permit three beams to be cast end to end. The sequence of operations in casting the test specimens was as follows: tensioning the strands, positioning the web reinforcement, form erection, casting, curing, form removal, instrumentation, and prestress release.

Two 50-ton mechanical jacks were used to tension the strands to approximately the desired value of 113.4 kips. A special hydraulic jacking arrangement was subsequently used to adjust the tension in individual strands if required.

Wire ties were used to secure the web reinforcement to the strand. In addition, it was found necessary to use a wire tie between successive projecting elements of the

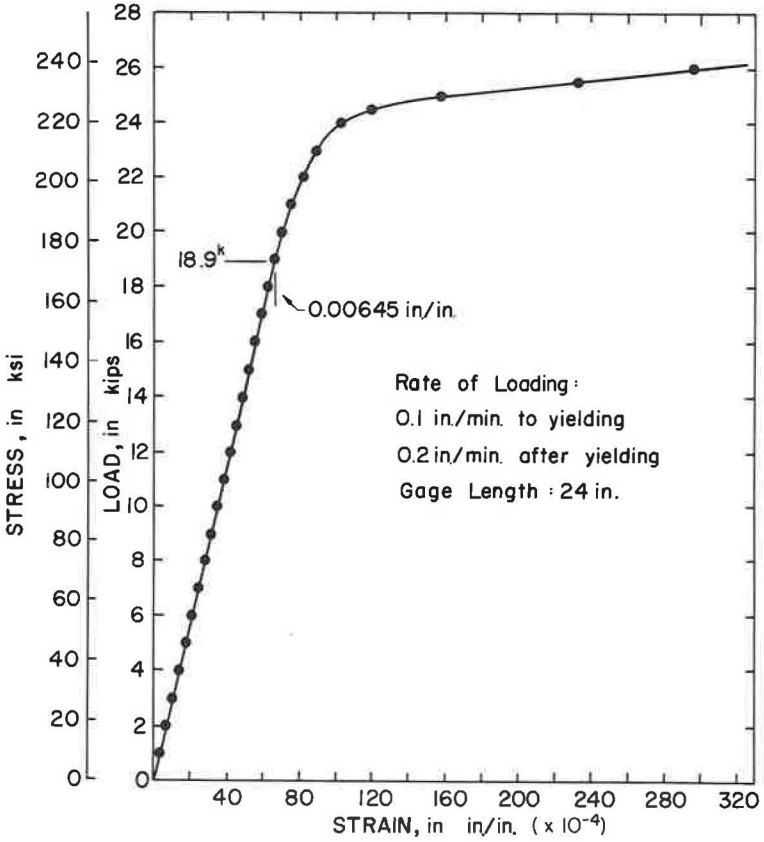

Figure 2. Stress-strain curve for prestressing strand.

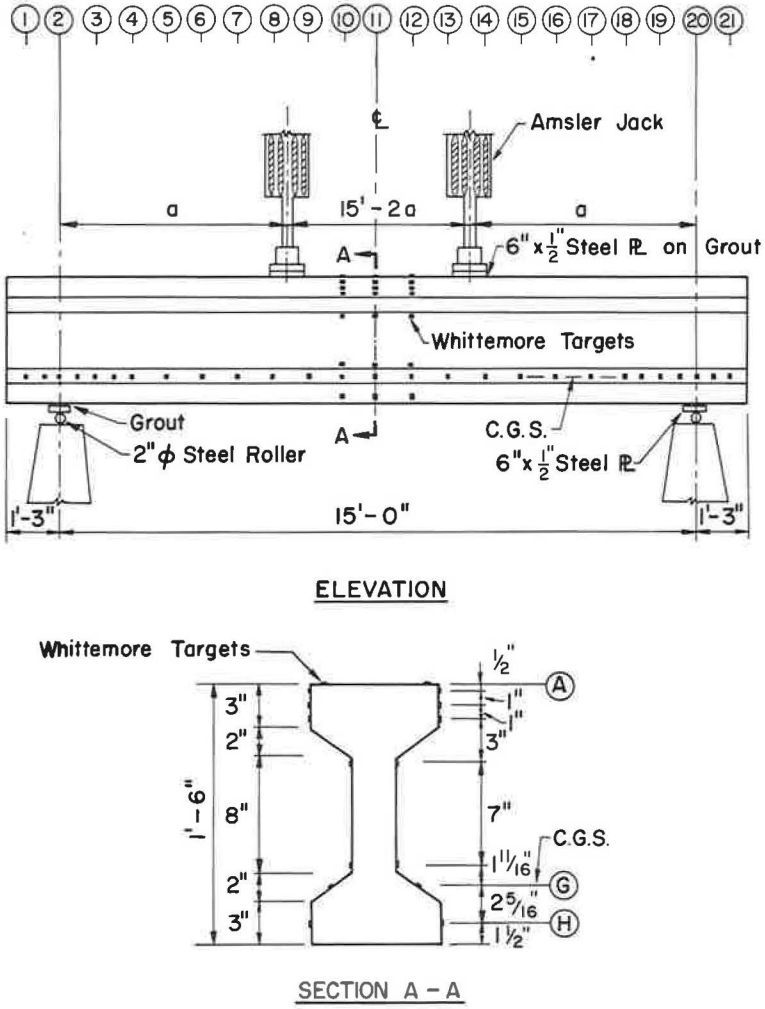

Figure 3. Test setup and principal instrumentation.

stirrups, in the compression flange area, to prevent movement of the stirrups during the casting operation.

Wood forms were used to cast the test beams. Dimensional checks made on the finished product indicated that, in general, dimensions were maintained within $\frac{1}{8}$ in., and consequently, the nominal dimensions of the cross-section given in Figure 1 were used in all calculations. With each test beam were cast six or more cylinders and three modulus of rupture beam specimens. Vibrators were used to place the concrete in both the test beams and the modulus of rupture specimens; the cylinders were rodded.

All specimens were covered with wet burlap and plastic sheeting for 5 days, after which the forms were stripped. Whittemore targets were positioned on the test beams on the sixth day. On the seventh day after casting, the prestress force was slowly released into the beams. The specimens were subsequently stored in the laboratory until the time of testing.

Instrumentation and Loading Apparatus

The test setup and principal instrumentation employed on the test beams is indicated in Figure 3. Loads for all test beams were symmetrically applied using two 55-kip Amsler hydraulic jacks bolted to a steel test frame. Vertical deflections were measured by both Ames dial gages and level readings. Deformation data were taken using a 10-in. Whittemore strain gage. The Whittemore targets were cemented to the test beams with an epoxy resin.

PROCEDURE AND RESULTS

Properties of the Concrete

Standard 6- by 12-in. cylinder tests were conducted to determine the ultimate compressive strength of the concrete associated with the test beams at the time to prestress release, f'_{ci}, and at the time of test, f'_c. Strains were measured on selected cylinders with a compressometer to determine the modulus of elasticity of the concrete, E_c. For comparison, values of E_c were also determined from the load deflection curves of the test beams. As a measure of the tensile strength of the concrete, the modulus of rupture, f'_r, was determined from 6- by 6- by 36-in. beams loaded at the third points of a 30-in. span.

Cylinder tests associated with prestress release were always carried out on the same day that the prestress force was released, usually within an hour or two of the actual operation. Cylinder and modulus of rupture tests associated with the beam test were carried out either on the same day, or in a very few instances, on the day after testing. The values of f'_{ci}, f'_c, f'_r, and E_c determined from these tests are given in Table 2. In general, each value is an average of three tests. As a typical example, the results of three cylinder tests associated with E. 5 at the time of test are shown in Figure 4.

Prestress Data

The initial strand tension was measured just before casting by load cells placed on each strand. The total initial prestress force, F_i, obtained for each test beam is given in Table 3.

Whittemore readings were taken along line G shown in Figure 3 to determine the elastic and inelastic losses in the prestress force, and the distance from the ends of the test beams, at the level of the center of gravity of the prestressing strand (c.g.s.), to the point at which 85 percent of the prestress force was effective. Readings were taken just before releasing the prestress force, after release, and again just before testing. The difference between these readings, converted to concrete strain, was plotted against location along the length of the test beam, a typical example of which is shown for E. 5 in Figures 5a and 5b.

Assuming that the concrete strain measured on the surface of the test beam at the level of the c. g. s. is equal to the average strain loss in the prestressing strand, the loss in the prestress force can be determined from the stress-strain curve of the strand. The

TABLE 2

PROPERTIES OF CONCRETE[a]

Beam	At Transfer			At Test				
	Age (days)	f'_c (psi)	E_c^1 (ksi)	Age (days)	f'_c (psi)	f'_r (psi)	E_c^1 (ksi)	E_c^2 (ksi)
E.1	7	5.600	3,100	67	7,030	690	4,000	4,600
E.2	7	5,640	3,100	62	6,690	740	3,600	4,200
E.3	7	5,690	3,100	56	6,720	660	3,500	4,300
E.4	7	5,500	3,200	55	6,960	700	3,900	4,700
E.5	7	5,530	3,100	60	6,610	670	3,800	4,600
E.6	7	5,440	3,200	62	7,100	730	4,100	4,500
E.7	7	5,900	3,800	62	7,230	800	4,100	4,700
E.8	7	5,680	3,400	70	6,970	650	4,400	4,700
E.9	7	5,630	3,500	74	7,140	720	4,200	4,700
E.10F	7	6,160	3,600	228	7,360	950	4,400	5,100
E.11F	7	6,410	3,600	245	7,790	960	4,200	5,000
E.12	7	5,590	3,300	68	7,020	680	3,900	4,700
E.13	7	6,130	3,700	27	7,320	630	4,400	4,500
E.14	7	5,670	3,600	47	6,780	680	4,100	4,700
E.15	7	5,730	3,500	35	6,940	670	4,300	4,600
E.16	7	5,650	3,300	64	6,950	610	3,700	4,500
E.17	7	5,400	3,300	57	6,580	600	3,800	4,300
E.18	7	5,520	3,200	52	6,640	580	3,600	4,500
Avg	-	5,720	3,400	-	7,000	710	4,000	4,600

[a]Modulus of elasticity values are designated E_c^1 if determined from cylinder tests and E_c^2 if determined from load-deflection curve of test beam.

strain determined from the difference in the Whittemore readings before and after release of the prestress force was considered to be the elastic loss. Similarly, the strain determined from the difference in the readings after release of the prestress force and just before testing was considered to be the inelastic loss. The losses and the prestress force at test, F, for each beam are given in Table 3.

The distance from the end of the beam at the level of the c. g. s. to the point at which 85 percent of the prestress force was developed was determined by plotting the total concrete strain at the time of test along the length of the beam. An example of this is shown for E. 5 in Figure 5c. Transfer distances determined in this way for the test beams are given in Table 3.

Static Beam Tests

Load was symmetrically applied to the test beams in shear increments of 2 kips, except when near loads at which cracking was expected. In this case, the shear increment was reduced to 1 kip. Data taken during the test included primarily load-deflection reading, strain measurements by Whittemore readings, and a log of the loads at which flexural cracking, inclined cracking, and ultimate failure took place. In addition, crack patterns were marked on the test beams after the application of each load increment. After failure the test beams were photographed.

The principal results of these tests are presented in Table 4. Convenient parameters for comparing the two principal variables in this investigation, length of shear span and amount of web reinforcement, are tabulated as the shear-span-to-effective-depth

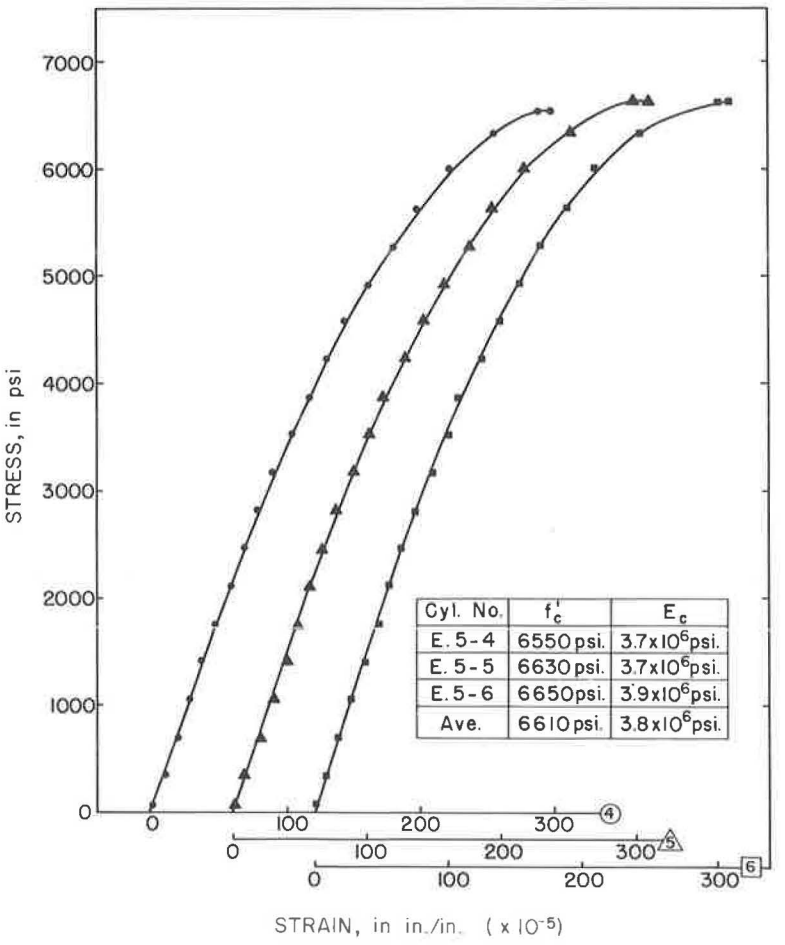

Figure 4. Cylinder tests for E.5 (at test).

TABLE 3
PRESTRESS DATA

Beam	F_i (kips)	Losses (%)			F (kips)	Transf. Dist. (in.)	
		Elastic	Inelastic	Total		End 2	End 20
E.1	113.7	8.4	12.9	21.3	89.4	11	9
E.2	113.7	8.5	12.7	21.2	89.5	12	14
E.3	113.7	9.0	12.3	21.3	89.4	14	17
E.4	113.9	8.8	11.3	20.1	91.0	11	12
E.5	113.9	8.6	11.9	20.5	90.6	14	14
E.6	113.9	8.5	12.3	20.8	90.2	16	16
E.7	114.9	8.1	11.8	19.1	92.0	13	15
E.8	114.9	8.1	11.8	19.9	92.0	14	15
E.9	114.9	8.1	12.7	20.8	91.0	17	15
E.10F	113.7	8.4	15.3	23.7	86.7	15	15
E.11F	113.7	8.3	15.4	23.7	86.7	14	16
E.12	113.7	8.5	12.3	20.8	90.0	12	15
E.13	113.5	7.8	7.1	14.9	96.6	15	14
E.14	113.5	7.6	7.3	14.9	96.6	10	11
E.15	113.5	7.3	7.9	15.2	96.3	13	11
E.16	113.3	8.2	11.0	19.2	91.6	13	15
E.17	113.3	8.4	10.2	18.6	92.4	14	13
E.18	113.3	8.5	9.9	18.4	92.6	15	15
Avg	113.8	8.3	11.5	19.8	91.4	13.5	14.0

ratio, a/d, and the web reinforcement index, $rf'_y/100$. The applied load shears at flexural cracking, inclined diagonal tension cracking, and at failure are given as V_c^f, and V_c^{dt}, and V_u, respectively.

Figures 6a and 6b show an overall view and a closer view of the right side, respectively, of E.12. The crack patterns are marked to indicate extent of cracking for the value of shear marked on the beam, and the dark lines marked on the web of the test beams, perpendicular to the longitudinal axis, indicate the location of the web reinforcement. The values of V_c^f and and V_c^{dt} can be readily determined from Figure 6b as 24 and 30 kips, respectively. The mode of failure is flexure.

Inclined diagonal tension cracking occurred in all of the test beams. This cracking was characterized by its sudden

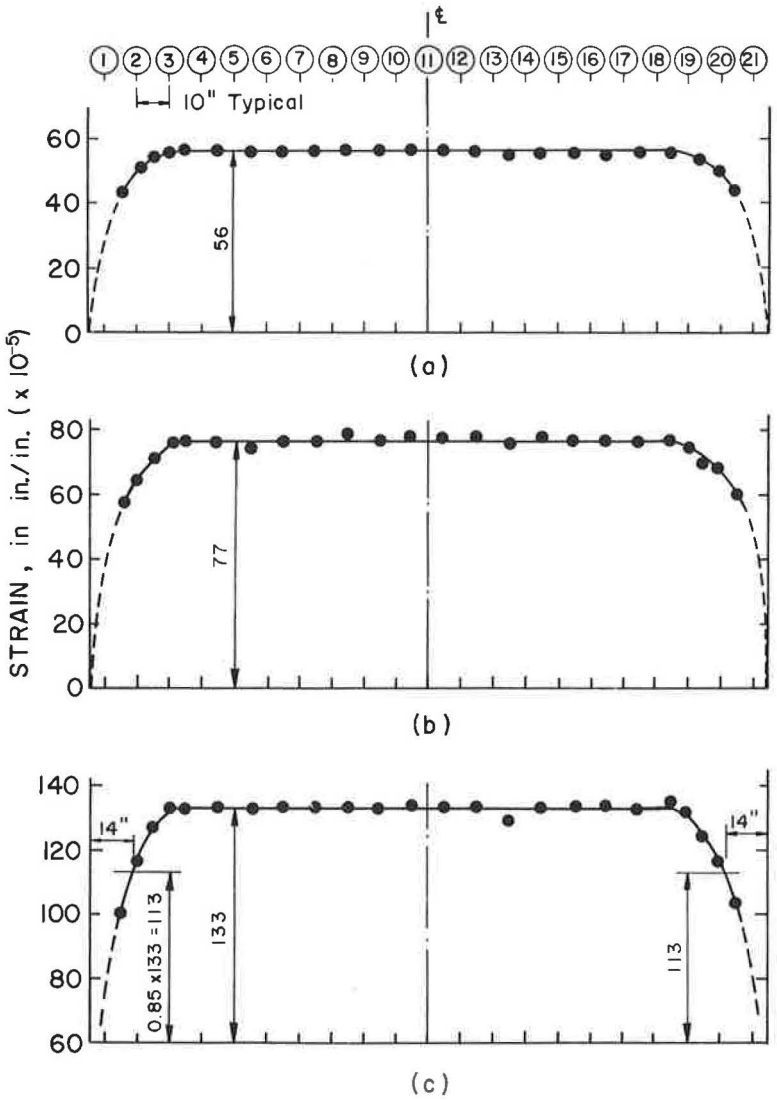

Figure 5. Concrete strain along c.g.s.: (a) after transfer, (b) from transfer to test, and (c) total strain to test.

appearance and by its initiation from an interior point in the web of the test beams. Because the hydraulic loading apparatus controlled the displacement introduced into the test beams and measured the corresponding applied force, a further characteristic of diagonal tension cracking was a noticeable drop-off in the measured applied load at the instant diagonal tension cracking formed.

In the test beams without web reinforcement, E.1 through E.4, the diagonal tension cracking load was, in effect, the ultimate load. Although the test beam did not collapse after the formation of diagonal tension cracking, failure appeared to be imminent. These four test beams were then unloaded and subsequently reloaded to failure. These final values of ultimate load are given as V_u in Table 4; however, the value of V_c^{dt} for these four test beams may be more appropriately regarded as the ultimate load.

The state of cracking in the test beams at the time of formation of the inclined diagonal tension cracks was reconstructed from photographs and is presented in the

TABLE 4

STATIC TEST RESULTS

Beam	$\frac{a}{d}$	$\frac{rf_y'}{100}$ (psi)	Shear, V (kips)				Nominal Shear Stress at Ult. Load $v_u = \frac{V_u}{b'd}$ (psi)	Mode of Failure[a]
			V_c^f	V_c^{dt} End 2	V_c^{dt} End 20	V_u		
E.1	6.34	0	14.4	-	20.4	16.2	381	S
E.2	5.07	0	16	-	23.9	20.8	489	S
E.3	4.23	0	20	26	-	23.1	542	S
E.4	3.39	0	24.4	30	-	30.8	724	S
E.5	3.39	676	24	31.8	28	42.0	988	F
E.6	3.39	508	24	30	28	41.8	984	F
E.7	3.39	406	25	28	28	41.1	965	F
E.8	3.39	339	23.3	28.2	27.2	41.2	968	F
E.9	3.39	254	24	28	28	41.2	968	F
E.10F	3.39	339	24	30	30	-	-	-
E.11F	3.39	254	24	30	28	-	-	-
E.12	3.39	204	24	30	30	41.2	968	F
E.13	3.39	222	24	30.6	29.2	41.7	981	F
E.14	2.54	222	33	33.8	32.3	53.8	1263	S
E.15	2.54	222	32	33	34	55.7	1310	F
E.16	3.39	162	24	30	30	39.9	939	F
E.17	3.39	121	24	26	29.4	38.0	894	S
E.18	3.39	97	24	27.1	31.5	38.7	911	S

[a] F = flexure; S = shear.

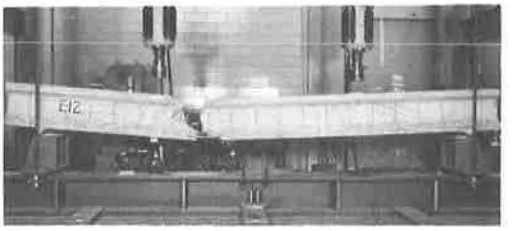

(a)

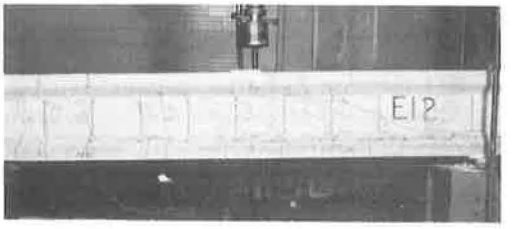

(b)

Figure 6. E.12 after failure: (a) elevation view, end 2 on right; and (b) end 2.

Appendix for selected test beams. Similar sketches of all of the test beams have been published previously (1). Diagonal tension cracking occurred on only one end of the test beams without web reinforcement because the diagonal tension cracking load was the ultimate load. Those beams with web reinforcement, however, had substantial load-carrying capacity beyond diagonal tension cracking; consequently, diagonal tension cracking would form, at different loads, in both shear spans.

In the figures in the Appendix, all cracking before the formation of diagonal tension cracking is indicated by solid heavy lines. The suddenly appearing diagonal tension cracking is indicated by dashed heavy lines, and the shear causing this cracking is indicated at the load point. Also shown in the figures, in the conventional way, is the location of the vertical web reinforcement.

The principal tensile stresses, σ_t, shown in the figures in the Appendix were

calculated, assuming an uncracked section and using the properties of the transformed section, at the intersection of the grid lines within the shear span and the junction of the web and top flange, the center of gravity, and the junction of the web and bottom flange. It was assumed that the state of stress was defined by a horizontal normal stress, σ, and a shearing stress, τ, and that the vertical normal stress was zero. Therefore, σ_t was calculated from the equation:

$$\sigma_t = \sqrt{\left(\frac{\sigma}{2}\right)^2 + \tau^2} + \frac{\sigma}{2} \qquad (1)$$

in which the normal stress was calculated from:

$$\sigma = F\left(\frac{ey}{I} - \frac{1}{A}\right) - \frac{y}{I}\left(V_c^{dt}x + M_d\right) \qquad (2)$$

and the shearing stress was calculated from:

$$\tau = \frac{Q}{Ib'}\left(V_c^{dt} + V_d\right) \qquad (3)$$

In Eq. 2, x is the horizontal distance from the reaction and y is the vertical distance, positive upwards, from the center of gravity of the transformed section. The slope of the compressive stress trajectory was calculated from the equation:

$$\theta = \frac{1}{2}\tan^{-1}\left(\frac{2\tau}{\sigma}\right) \qquad (4)$$

Light dashed lines in the shear span show the compressive stress trajectories in the web of the test beams.

For some test beams, for example, E.14, there was no cracking in the shear span before diagonal tension cracking and, therefore, the given principal stresses represent the state of stress just before cracking. However, for other test beams, for example, E.3, inclined cracking which began as a flexural crack occurred in the shear span before diagonal tension cracking. Therefore, the calculated principal stresses in the region of the flexural cracking do not accurately represent the state of stress at the time of diagonal tension cracking.

Examination of the inclined cracking indicated that three test beams, E.1, E.2, and E.3, had a lower value of the inclined cracking load than the value of V_c^{dt} given in Table 4. These three test beams are shown in Figure 7. Inclined cracks may be seen which begin as flexural cracks but, because of the presence of shear, turn and become inclined in the direction of increasing moment. Inclined cracks of this type will be called flexure shear

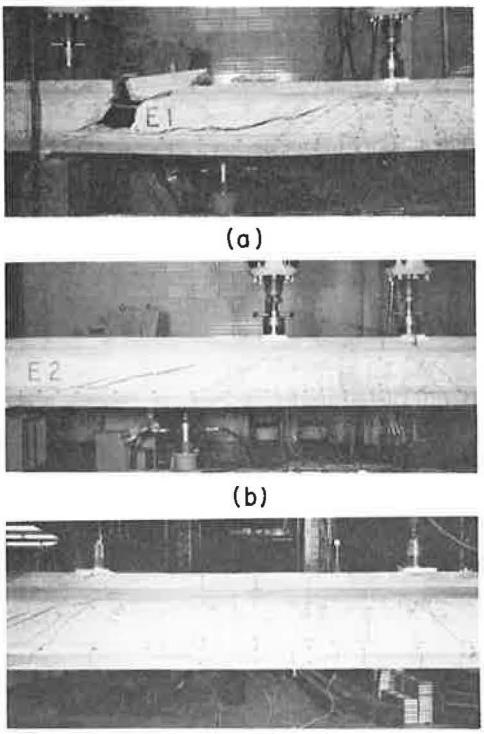

Figure 7. Beams after failure: (a) E.1, (b) E.2, and (c) E.3.

TABLE 5

SHEAR AT FLEXURE SHEAR CRACKING

Beam	a/d	V_c^{fs} (kips)
E.1	6.34	17.5
E.2	5.07	22
E.3	4.23	26

cracks and will be considered significant when they occur at a distance equal to or greater than the effective depth of the beam outside of the concentrated load point with which they are associated. From these figures, values of applied load shear, V_c^{fs}, in agreement with the definition of significant flexure shear cracking were determined; the values selected are given in Table 5. The value of V_c^{fs} equal to 26 kips for E. 3 is the same as the value of V_c^{dt} given in Table 4. In this case, the diagonal tension crack formed while holding the load on E. 3 constant at a shear of 26 kips. A significant flexure shear crack, however, had formed just before reaching the shear of 26 kips.

Modes of failure of the test beams were classified in Table 4 as flexure or shear. The flexural failures were all similar, being characterized by crushing of the concrete in the compression zone and sudden complete collapse of the test beam. Test beam E. 5 (Fig. 8) may be regarded as typical of the flexural failures.

The shear failures were dissimilar. In the beams without web reinforcement, E. 1 through E. 4, as previously noted, the formation of diagonal tension cracking caused the beam to appear unstable but did not trigger a collapse mechanism. Subsequent unloading and reloading to failure led to a collapse mechanism characterized in all four cases by crushing of concrete in the lower portion of the web and by the simultaneous development of a tension crack in the top flange. The failure in E. 4 typifies this description. The failure in test beams E. 1 through E. 3 was similar to that shown in Figure 9 for E. 4, and the failure region in all cases was located approximately the effective depth of the test beam from the reaction.

(a)

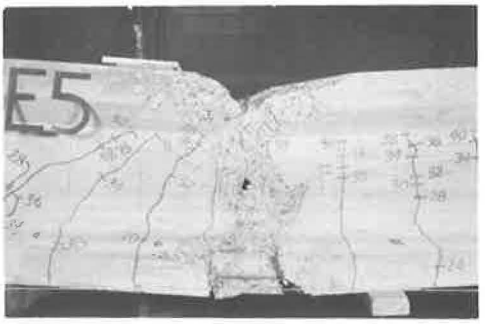

(b)

Figure 8. Flexural failure in E.5: (a) elevation view, end 2 on right; and (b) failure region.

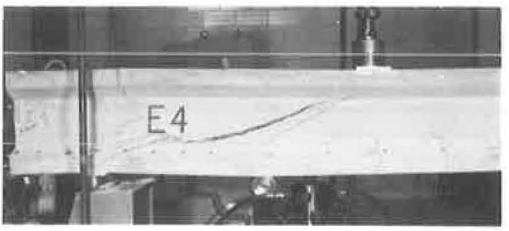

Figure 9. Shear failure in E.4.

Two beams with web reinforcement, E. 17 and E. 18, failed in shear. Overall and close-up views of the shear span in which the failure occurred are shown for both of these beams in Figures 10 and 11, respectively. Only the close-up view of E. 18 is taken (Fig. 11b) in the test setup. The other three pictures were taken after the beams were removed from the test setup, and artificial means are used to indicate the location of the reactions and load points.

The shear failure in E. 17 was gradual and nonviolent, being characterized by crushing of concrete in the web. No stirrups were broken. In contrast, the shear failure in E. 18 was sudden and violent. Examination of E. 18 after failure showed that the second and third stirrup from the reaction had fractured.

As previously noted, beams E. 13 and E. 14 had inverted L-shaped stirrups for web reinforcement, in contrast to the U-shaped stirrups used in the other test beams. Beam E. 13 failed in flexure. However, E. 14 failed in shear due to a bond failure in the web

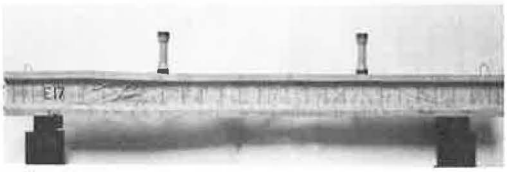

(a)

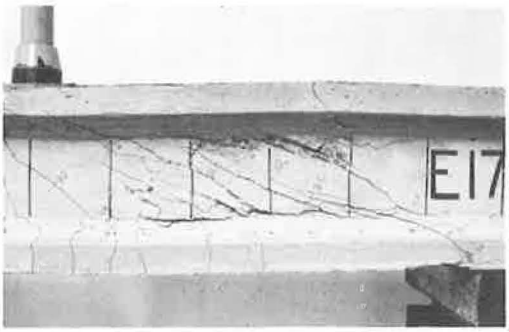

(b)

Figure 10. Shear failure in E.17: (a) elevation view, end 2 on left; and (b) opposite side of failure region.

(a)

(b)

Figure 11. Shear failure in E.18: (a) elevation view, end 2 on right; and (b) failure region.

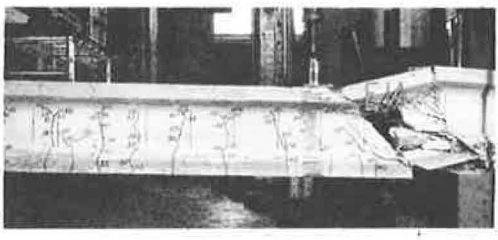

(a)

(b)

Figure 12. Failure in E.14: (a) part elevation view, end 20 on right; and (b) failure region.

reinforcement. As can be seen from the close-up view of the failure region in Figure 12, the second stirrup from the reaction had inadequate anchorage below the point at which it was crossed by an inclined crack to develop the strength of the stirrup, thereby triggering the shear failure.

Strain measurements were taken at selected intervals during the course of a beam test. As shown in Figure 3, the Whittemore targets can be separated into two groups. The first group may be considered to consist of the set of targets on the c.g.s., i.e., on the horizontal line G, and the second group to consist of the set of targets on vertical lines 10, 11, and 12.

The first group of targets was intended, in addition to determining prestress losses, to show the variation in concrete deformation with applied load along the c.g.s. Accordingly, strain data for E.16, which failed in flexure, and E.17 and E.18, which failed in shear, are presented in Figures 13, 14, and 15, respectively.

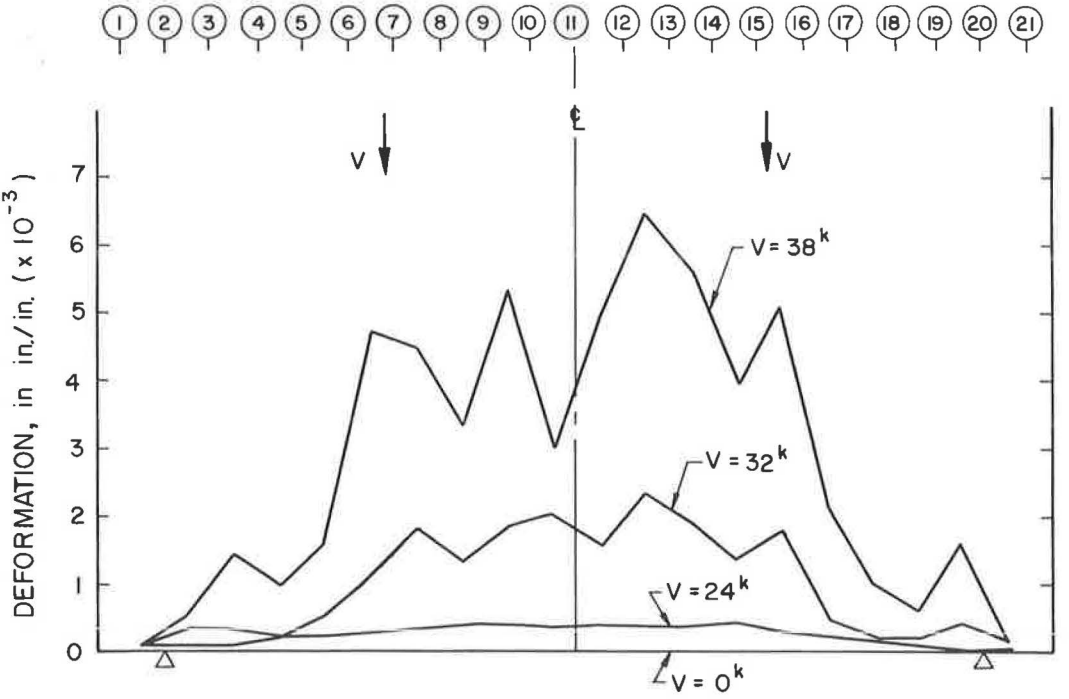

Figure 13. Concrete deformation along c.g.s. during test of E.16.

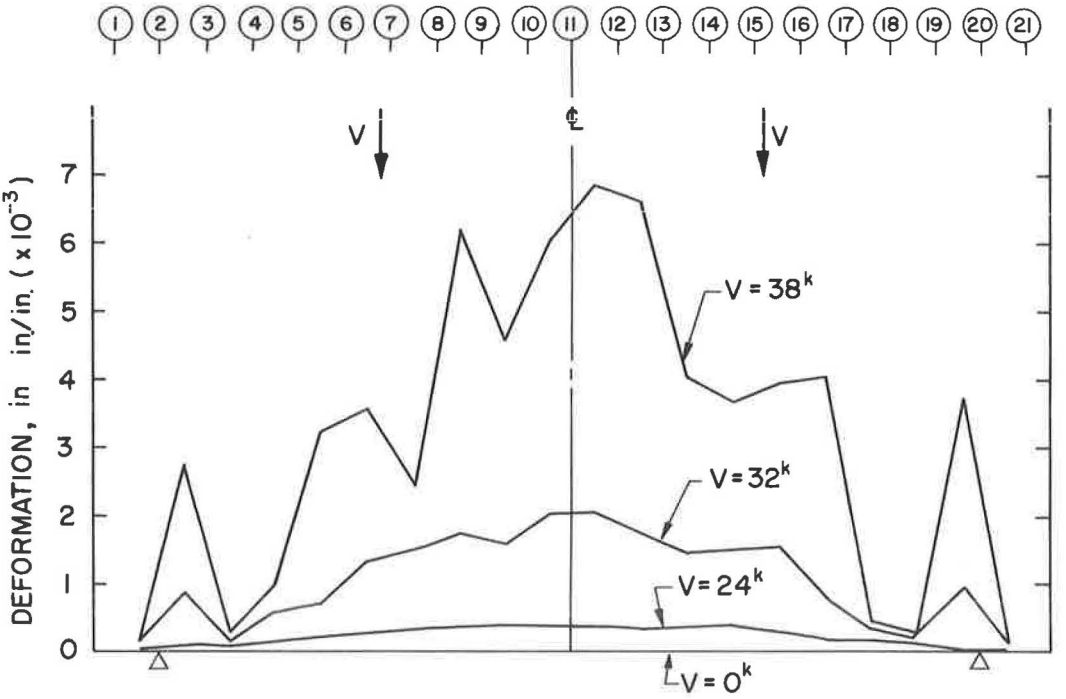

Figure 14. Concrete deformation along c.g.s. during test of E.17.

Data taken for the other test beams are not reported. In these figures, the variation in concrete deformation along the c.g.s. is given for three values of shear; 24, 32, and 38 kips. For all three test beams, the flexural cracking load, V_c^f, was equal to 24 kips; therefore, the deformation at this load may be regarded as concrete strain. At V = 32 kips, inclined diagonal tension cracking had occurred for all three beams, and flexural cracking had extended across the c.g.s. The deformations for V = 38 kips are, in all three cases, indicative of the deformations at ultimate load.

The second group of targets was intended to give the deformation at a vertical section in the constant moment region of the test beams. Test beam E. 5 may be regarded as typical; the data for this beam are plotted in Figure 16. Each plotted point is an average of readings between lines 10 and 11 and 11 and 12 on both sides of the member. This plot includes data taken before and after transfer, as well as before and during the test. In Figure 16, the strains before and after transfer, from transfer to test, and during the test are plotted separately; e.g., the strain from after transfer to test is measured between the vertical zero line and the indicated line.

In Figure 17, the data in Figure 16 have been used to determine the elastic strain distribution in E. 5 just before testing, i.e., at V = 0, and corresponding to selected magnitudes of shear during the test. The strain distribution determined from the Whittemore readings before and after transfer was assumed to be elastic strain. This was corrected to indicate the elastic strain just before testing by evaluating the effect of the change in prestress force due to the inelastic losses occurring from after transfer to time of test. The deformation corresponding to the different increments of shear were then added to the elastic strain at V = 0. From Figure 17, the strain in the top fibers of the test beams, ϵ_u, and the approximate location of the neutral axis at failure can be determined by extrapolation to the ultimate load, V_u, equal to 42.0 kips.

Values of ϵ_u, determined as indicated in the preceding paragraph, and ultimate moment, M_u, are given in Table 6 for those test beams failing in flexure. The values

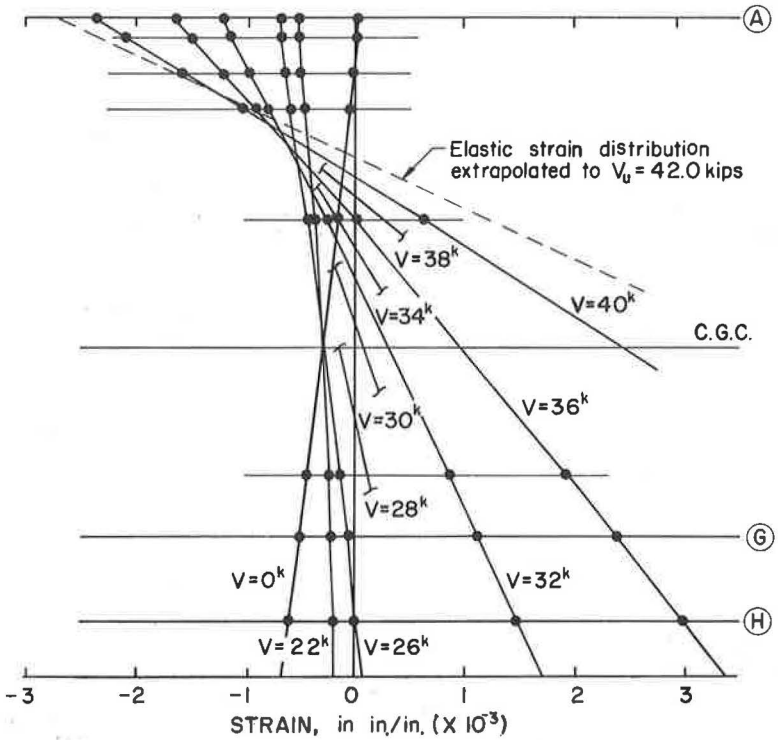

Figure 17. Elastic strain history of E.5.

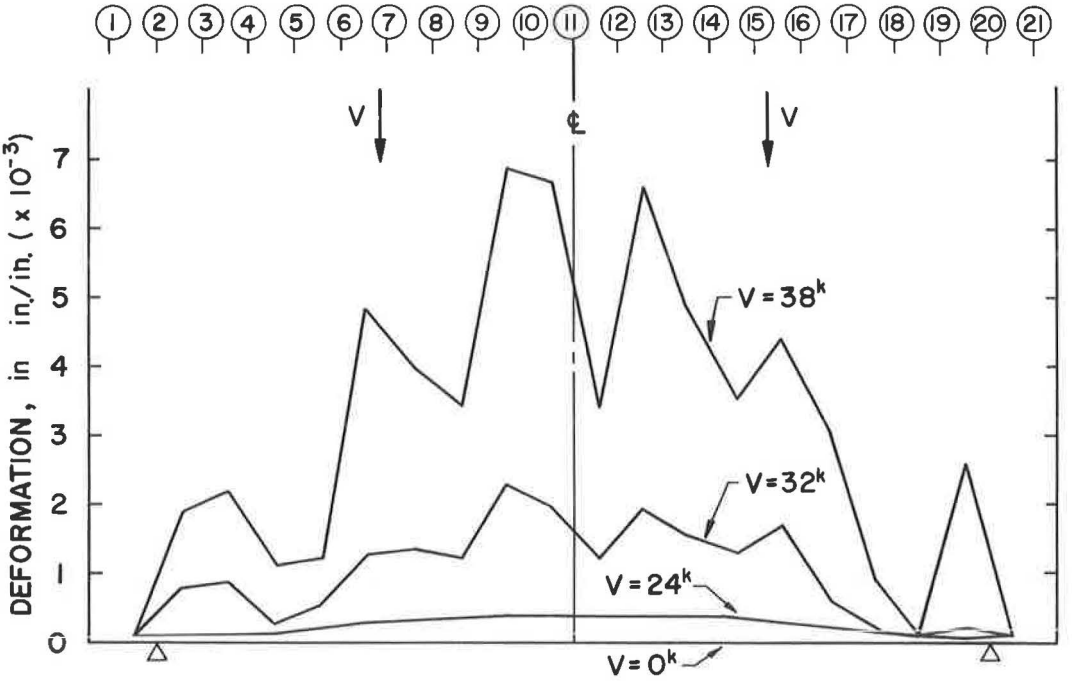

Figure 15. Concrete deformation along c.g.s. during test of E.18.

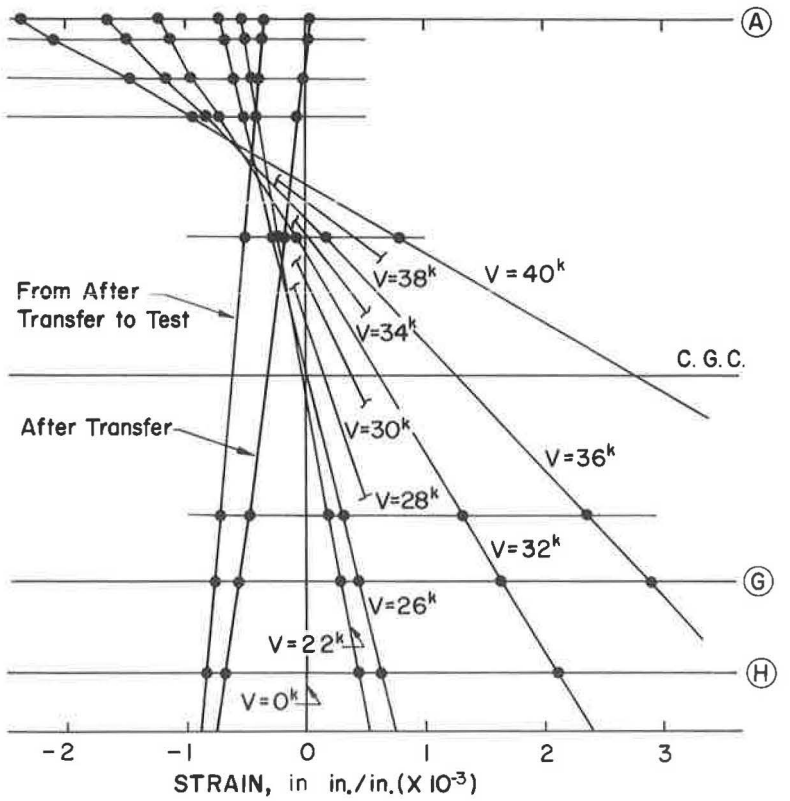

Figure 16. Strain distribution of E.5.

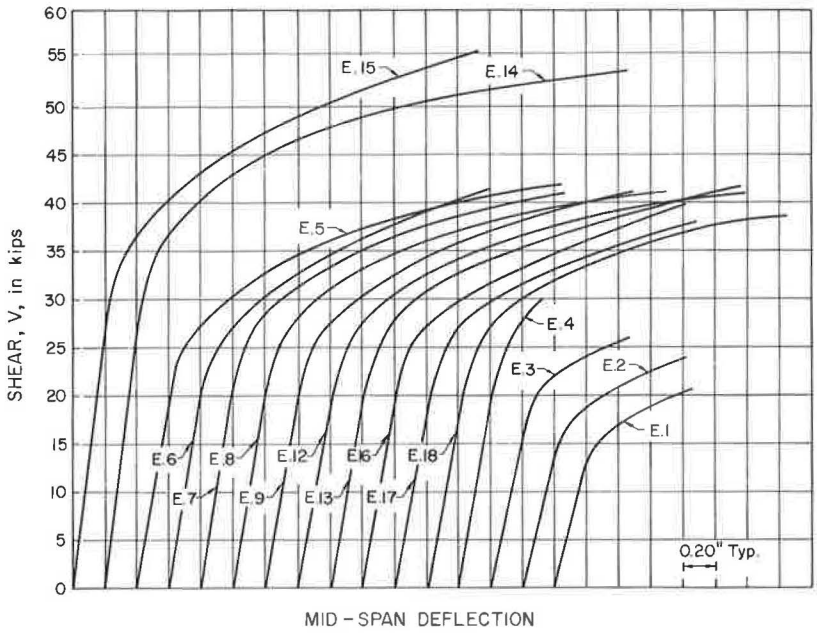

Figure 18. Load-deflection curves for test beams.

TABLE 6

BEAMS FAILING IN FLEXURE

Beam	ϵ_u (in./in.)	M_u (kip-ft)
E.5	0.0027	170.9
E.6	0.0027	170.1
E.7	0.0028	167.3
E.8	0.0025	167.7
E.9	0.0025	167.7
E.12	0.0028	167.7
E.13	0.0025	167.7
E.15	0.0025	170.0
E.16	0.0028	162.5

of M_u include an allowance of 2.9 kip-ft for dead load moment. The average experimental ultimate moment of these nine beams was 168.2 kip-ft. For comparison, the calculated ultimate flexural capacity according to Section 1.13.10 of the AASHO specification, assuming f'_c = 7,000 psi (average f'_c of all test beams) and f'_s = 252.5 ksi, was 164.5 kip-ft.

Load-deflection curves for the static tests are presented in Figure 18.

DISCUSSION

Overload Behavior of Prestressed I-Beams

Knowledge of the ultimate strength of a prestressed beam requires an understanding of the physical behavior of this type of member under load. This behavior may be described with reference to the uncracked or cracked loading range.

In the uncracked range, the familiar formulas of structural mechanics, based on an uncracked section and a linear strain distribution, are applicable. However, at cracking a fundamental change takes place in the way in which the prestressed beam carried load. Two cases are important. Where flexure predominates, the strain distribution remains linear after cracking up to failure. With this as a compatibility condition, the ultimate flexural capacity can be accurately determined. Where shear is significant, inclined cracks develop in the prestressed beam. In the zone of inclined cracking, the strain distribution is nonlinear. If shear is critical, the inclined cracking leads to a shear failure.

The ultimate shear strength of prestressed concrete members has been studied extensively in recent years. Three important conclusions may be drawn from these investigations:

1. The inclined cracking load in a prestressed beam without web reinforcement is the same as the inclined cracking load in a prestressed beam with web reinforcement;
2. The inclined cracking load in a prestressed beam without web reinforcement and subjected to moving loads is the ultimate load; and
3. The stress in web reinforcement is not significant unless crossed by an inclined crack.

Tests on 33 pretensioned I-beams without end blocks by Hulsbos and Van Horn (2) may be regarded as a basis for the first conclusion. The results of their tests indicated that the amount of web reinforcement had no apparent effect on the magnitude of shear causing the formation of inclined cracks. This conclusion is supported by the results presented in Table 4. Comparison of the values of V_c^{dt} for beams tested on an a/d ratio of 3.39 shows no significant trend with amount of web reinforcement.

McClarnon, Wakabayashi, and Ekberg (3) conducted tests on two pretensioned beams of rectangular cross-section without web reinforcement which were first symmetrically loaded until fully developed flexure shear cracking had occurred. The two beams were then unloaded and subsequently reloaded to failure on an increased shear span. The ultimate shear strength of the two beams was approximately equal to the shear causing significant inclined cracking in two other beams without the load points moved. The four E Series tests without web reinforcement, E.1 through E.4, also support the second conclusion, without the restriction that the loads be moving loads. As indicated in Table 4, the maximum shear sustained by these beams was either equal to or nearly equal to the shear causing diagonal tension cracking.

Work by Mattock and Kaar (4) on the shear strength of continuous prestressed girders with web reinforcement forms a basis for the third conclusion. Their investigation showed that before diagonal tension cracking, the web reinforcement was only slightly stressed, in either tension or compression. With diagonal tension cracking, web reinforcement crossed by the cracking yielded immediately.

The importance of the three conclusions discussed in the preceding paragraphs emphasizes the need to determine accurately the inclined cracking strength of a prestressed beam. There is first the flexure shear type of inclined cracking, which begins as a flexure crack but, because of the presence of shearing forces, becomes inclined in the direction of increasing moment. An important characteristic of this type of cracking is that its development is more rapid than a flexural crack. Therefore, the flexure shear inclined cracking load at a particular section may be realistically taken as the load which will cause a flexural crack to form first at some distance in the direction of decreasing moment from this section. The distance from the section must be sufficient to permit the development of a significant inclined crack which would lead to a critical shear condition.

Hulsbos and Van Horn (2) determined that the principal stress method was satisfactory for evaluating the diagonal tension cracking strength of pretensioned I-beams. Their conclusion was based on a study of the calculated state of stress in the web of the I-beam just before inclined cracking, and included an approximation of the stresses due to the stress concentration from the reaction and load point. The inclined cracking load was calculated as the load causing the principal tensile stress to reach a certain limiting value at any point in the web of the I-beam.

A very thorough study of the shear at inclined cracking of a large number of prestressed beams has been made by Hernandez, Sozen, and Siess. Their design proposals, based on the findings of this study, have been summarized by Mattock and Kaar (4) and state that the shear at inclined cracking shall be taken as equal to the least shear which will produce either of the following effects: (a) a net tensile stress of $6\sqrt{f_c'}$ in the extreme fiber in tension at a distance from the section considered equal to the effective depth of the section, measured in the direction of decreasing moment; or (b) a principal tensile stress of $4\sqrt{f_c'}$ at the intersection of the neutral axis with a 45° line drawn in the direction of decreasing moment from the extreme fiber in compression of the section considered.

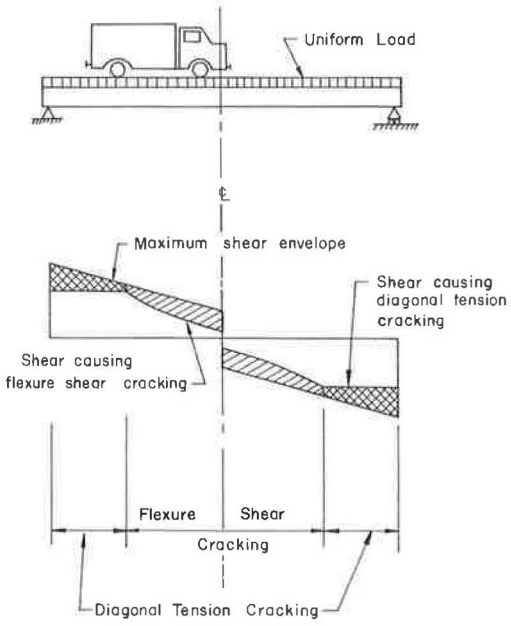

Figure 19. Behavior of simply supported prestressed beam with web reinforcement.

The significant feature of the proposals by Hernandez, Sozen, and Siess is that only the state of stress at the neutral axis of the member is considered in determining the inclined diagonal tension cracking load. Inasmuch as the state of stress at the bending neutral axis is simplified because flexural stresses are zero at that point, the inclined cracking load becomes a function of only two variables, the limiting tensile strength of the concrete and the effective prestress force, and can be readily calculated.

The discussion in the preceding paragraphs can form the basis of a consideration of the behavior of a simply supported prestressed beam with web reinforcement, as shown in Figure 19, subjected to a uniform load and a moving vehicle load. These applied loads can represent design loads multiplied by appropriate load factors, i.e., ultimate loads. The crack patterns may develop in several ways. For beams with the greater span lengths, the first cracking would be flexural, followed by flexure shear cracking. For intermediate span lengths, diagonal tension cracking may either precede or follow flexure shear cracking. For short span lengths, diagonal tension cracking may precede flexural cracking.

If the span is regarded as being of intermediate length, both flexure shear and diagonal tension cracking must be considered. Wherever the shear in the beam produces a stress in the web equal to the principal tensile strength of the concrete, or a stress in the bottom fibers equal to the flexural tensile strength of the concrete, diagonal tension or flexure shear cracking, respectively, may occur. A plot of the least value of shear causing either diagonal tension or flexure shear cracking on a diagram of the maximum shear envelope, as in Figure 19, indicates the amount of shear which must be carried at any section after inclined cracking. Because the web reinforcement does not begin working until an inclined crack forms, the amount of shear carried after inclined cracking must be a function of the amount of web reinforcement in the beam.

A section arbitrarily located in the beam in Figure 19 in the region where inclined cracking would exist is shown in Figure 20. A free body diagram of the portion of the beam to the left of this section may be drawn by separating the beam along the path of an inclined crack, say JK, and by a vertical cut through the concrete at the top of the inclined crack, say KL. Because the path of the inclined diagonal tension crack will not extend through to the bottom flange in the region of J, the section taken along JK may pass through some concrete. The principal forces at this section would be the two components of the resultant force in the strand, F_H and F_V, the two components of the resultant force in the web reinforcement, V_{w_H} and V_{w_V}, and the resultant force transmitted through the concrete, which may be represented by a horizontal compressive force, C, and a shearing force, V_c. For prestressed beams with web reinforcement, the horizontal component of the force in the web reinforcement is small, and therefore, V_{w_V} may be taken as simply V_w. Likewise, the vertical component of shear transmitted across the prestressing elements is small and may be neglected. Thus, the general free body diagram may be replaced by a simplified free body diagram, also shown in Figure 20.

V_u can be considered the ultimate shear on this section located x distance from the support. For equilibrium:

$$V_u = V_c + V_w \qquad (5)$$

But V_w may be regarded as known, based on the assumption that web reinforcement crossed by an inclined crack has yielded. Therefore, if A_v is the area of a single stirrup and s is the spacing:

$$V_w = A_v f'_y \frac{\beta d}{s} \qquad (6)$$

in which f'_y is the yield point of the web reinforcement. Solving for A_v gives the equilibrium requirement that:

$$A_v = \frac{\left(V_u - V_c\right) s}{f'_y \beta d} \qquad (7)$$

Eq. 7 has several significant features. If V_c and β were known, the form of Eq. 7 is such that it could readily be used as a design equation. In fact, with $\beta = 1$, Eq. 7 has been presented as a design proposal by Hernandez, Sozen, and Siess (4), in which V_c is assumed equal to the inclined cracking load and is calculated according to the recommendations previously given. Mattock and Kaar (4) have also presented a design equation of the form of Eq. 7, in which V_c is calculated according to the recommendations of Hernandez, Sozen, and Siess and the factor β is taken equal to $3.5 \sin(\tan^{-1} a/d)$.

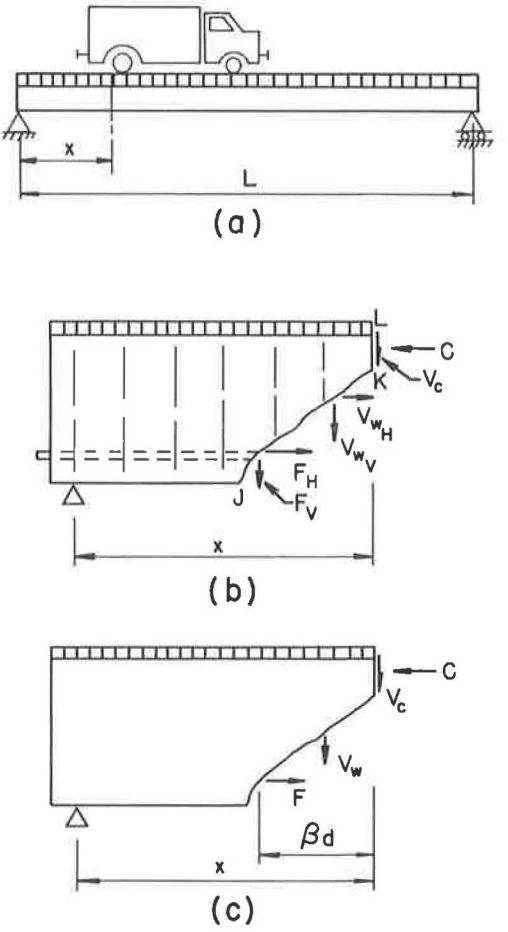

Figure 20. Shear equilibrium condition: (a) elevation, (b) general free body diagram, and (c) simplified free body diagram.

The assumption that the shear just before inclined cracking is equal to the shear carried by the concrete at failure is supported by the tests on E. 1 through E. 4. These four beams, all without web reinforcements, were initially loaded until inclined diagonal tension cracking formed, indicated in Table 4 as V_c^{dt}. At this point in the test, the beams, which had become very unstable, were unloaded. Subsequently, the beams were reloaded to failure, indicated as the shear V_u in Table 4. In the reloading process, essentially all of the shear must have been carried by the concrete in the region above the top of the inclined crack. The lowest ratio of V_u to V_c^{dt} is 0.80, in the case of the beam with the longest shear span; the average ratio for these four tests is 0.90. Furthermore, there is reason to believe that with even a small amount of web reinforcement, the crack opening in the web would have been restricted and the ratio of V_u to V_c^{dt} would have increased to 1 or greater.

The angle of inclination of the inclined crack, for diagonal tension cracking, is closely associated with the direction of the compressive stress trajectory, as can be readily seen from the crack patterns presented in the Appendix. Observations from the tests reported herein indicated that before failure would occur, the inclined crack would have developed sufficiently to have crossed all web reinforcement in its projected path. Therefore, β may be calculated as the factor which, when multiplied by d, gives the horizontal projection of an inclined crack with inclination approximated as the slope

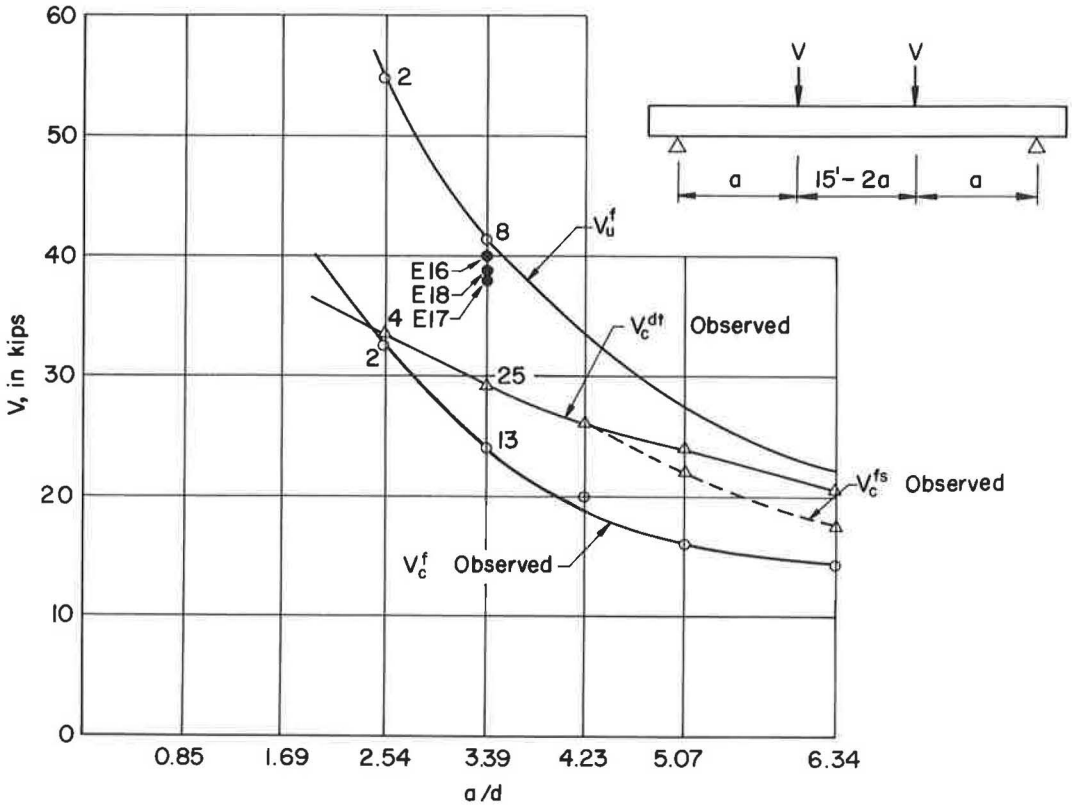

Figure 21. Static strength of test beams.

of the compressive stress trajectory at the bending neutral axis, and arbitrarily considered to extend from the junction of the web and the top flange to the lowest depth at which the web reinforcement may be regarded as effective. This may be expressed as:

$$\beta = \frac{\ell_e}{(\tan\theta)\, d} \tag{8}$$

in which ℓ_e is the distance from the intersection of the top flange and web to the lowest point at which the web reinforcement may be regarded as effective.

For flexure shear cracking, β could have values varying from 0 to greater than 1. Experimental observations indicated that flexure shear cracks forming at β values of less than 1 are supplanted by more critical flexure shear cracks with values of β greater than 1. Therefore, it is conservative to take $\beta = 1$ for all flexure shear cracking.

With V_c and β values determined according to the discussion in the preceding paragraphs, Eq. 7 becomes a criterion for proportioning vertical web reinforcement in a prestressed beam. But Eq. 7 has limitations as an ultimate shear strength equation. The purpose of web reinforcement is to permit an increase in the load-carrying capacity of the beam above the inclined cracking load. This is accomplished by effecting a redistribution of forces in the beam at inclined cracking. In effect, the beam action destroyed by inclined cracking must be restored by web reinforcement. The conditions required to insure that this restoration of beam action takes place must be met before Eq. 7 can be regarded as having any meaning; these conditions include limitations on the spacing of the web reinforcement, anchorage and bond requirements, which can be summed up under the heading of good dimensional proportioning. Assuming that the conditions required for the redistribution of forces are met, the prestressed beam

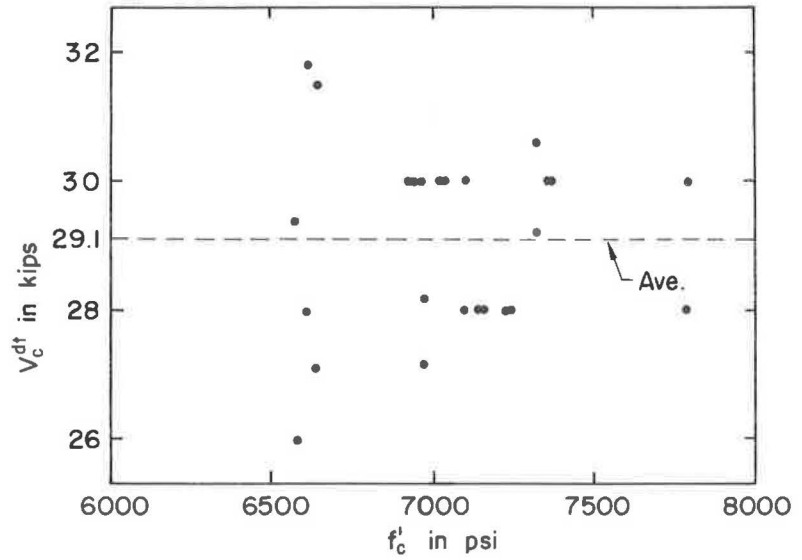

Figure 22. Variation in V_c^{dt} with concrete strength for a/d = 3.39.

critical in shear may fail in three ways: (a) by fracture of the web reinforcement, (b) by web distress, i.e., by crushing of concrete in the web, and (c) by shear compression. But if failure occurs as fracture of the web reinforcement, the critical stress would be the ultimate stress, f_u', which may be more than 50 percent greater than f_y'. Similarly, failure due to web distress or shear compression must be associated with the strength of the concrete. None of these indices, however, are an explicit part of Eq. 7.

Static Shear Strength of Test Beams

The preceding section discussed the overload behavior of prestressed I-beams with web reinforcement. The purpose of this section is to correlate the test results with the discussion in the preceding section.

For this purpose, the test results given in Tables 4 and 5 are plotted as applied load shear, V, vs the a/d ratio on which the test was conducted, as shown in Figure 21. In this form, the results represent the experimentally determined flexural cracking, inclined cracking, and ultimate strength of the type of member being tested. The number beside some of the plotted points indicates the number of tests for which that point is an average.

The test beams ranged in concrete strength from 6,580 to 7,790 psi; the average value of f_c' was 7,000 psi. The effective prestress force ranged from 86.7 to 96.6 kips; the average value of F was 91.4 kips. The 25 points, plotted as an average in Figure 21, indicating the diagonal tension cracking strength of the test beams on an a/d ratio of 3.39 are plotted as individual points in Figure 22 and indicate little variation in inclined cracking strength with concrete strength over the small range of concrete strengths being considered. Similarly, the flexural capacities of the static test beams failing in flexure, presented in Table 6, do not indicate any significant variation with concrete strength or prestress force. Therefore, the data plotted in Figure 21 may be regarded as representing an "average" test beam with a concrete strength of 7,000 psi and a prestress force of 91.4 kips.

The flexural cracking moment of the test beams would generally be calculated from the equation:

TABLE 7

FLEXURAL TENSILE STRENGTH AND PRINCIPAL TENSILE STRENGTH DETERMINED FROM TEST BEAMS

Beam	f_t' (psi)	$f_t'/\sqrt{f_c'}$	σ_t^{cg} (psi) End 2 (psi)	σ_t^{cg} (psi) End 20 (psi)	$\sigma_t^{cg}/\sqrt{f_c'}$ End 2	$\sigma_t^{cg}/\sqrt{f_c'}$ End 20
E.1	-a	-	-b	-c	-	-
E.2	710	8.68	-b	-c	-	-
E.3	-a	-	-c	-b	-	-
E.4	725	8.70	435	-b	5.22	-
E.5	690	8.49	480	395	5.90	4.85
E.6	695	8.26	445	405	5.29	4.81
E.7	765	9.00	395	395	4.65	4.65
E.8	585	7.01	405	375	4.86	4.50
E.9	680	8.04	400	395	4.74	4.68
E.10F	760	8.85	450	455	5.24	5.30
E.11F	760	8.62	455	410	5.16	4.66
E.12	700	8.35	440	445	5.25	5.31
E.13	565	6.60	440	410	5.15	4.80
E.14	640	7.77	480	500	5.83	6.08
E.15	570	6.84	490	520	5.88	6.25
E.16	665	7.97	440	440	5.28	5.28
E.17	655	8.08	355	425	4.38	5.24
E.18	645	7.82	370	475	4.54	5.83
Avg	675	8.07	430		5.16	

[a] Values of f_t' calculated for these beams regarded as unrealistically high and indicate that the corresponding experimentally determined values of V_c^f are too high.

[b] Diagonal tension cracking at other end only.

[c] Not applicable because of prior flexure shear cracking.

$$M_c^f = Z^b \left[f_t' + \frac{F}{A} + \frac{F(e)}{Z^b} \right] \quad (9)$$

Expressed in terms of the shear causing flexural cracking in the test beams, this equation becomes:

$$M_c^f = V_c^f(a) + M_d \quad (10)$$

Solving for f_t' yields,

$$f_t' = \frac{V_c^f(a) + M_d}{Z^b} - \frac{F}{A} - \frac{Fe}{Z^b} \quad (11)$$

Using Eq. 11, values of F from Table 3, and values of V_c^f from Table 4, f_t' was calculated, and the values determined are given in Table 7. M_d was taken as the maximum dead load moment, or 2.9 kip-ft. The average value of the flexural tensile strength determined in this manner was 675 psi, and corresponds to an average ratio of $f_t'/\sqrt{f_c'}$ of 8.07. The minimum ratio of $f_t'/\sqrt{f_c'}$ was 6.60, as determined for E. 13. Therefore, the recommendation of Hernandez, Sozen, and Siess that the critical tensile stress in the extreme fiber in tension be taken as $6\sqrt{f_c'}$ would have conservatively predicted the flexural cracking moment for all the E Series test beams. Their recommendation was based on an investigation which covered a much wider range of concrete strengths than were included in the E Series tests. However, Figure 23 shows a plot of f_c' vs $f_t'/\sqrt{f_c'}$, and indicates no significant trend in the range of concrete strengths investigated. Thus, for concretes similar to those tested in this investigation, the flexural tensile strength of the concrete may be determined as:

$$f_t' = 6.5\sqrt{f_c'} \quad (12)$$

The V_c^f design curve shown in Figure 24 was determined using Eq. 11, with f_t' calculated from Eq. 12, for an "average" test beam.

The calculated inclined cracking strength depends on whether the inclined cracking is classified as flexure shear or diagonal tension. With flexure shear cracking, assuming that the shear causing flexure shear cracking, V_c^{fs}, is equal to the shear causing a flexural crack to form a distance d from the load point:

$$V_c^{fs} = \frac{M_c^f - M_d}{a - d} \quad (13)$$

The V_c^{fs} design curve shown in Figure 24 was determined from Eq. 13. It is a conservative estimation of the V_c^{fs} observed curve, as it must be because the flexure shear cracking was not considered significant until it formed a distance d or greater away from the load point.

The transition from flexure shear to diagonal tension cracking may be seen, from Figure 21, to take place in the neighborhood of an a/d ratio of 4. From an examination

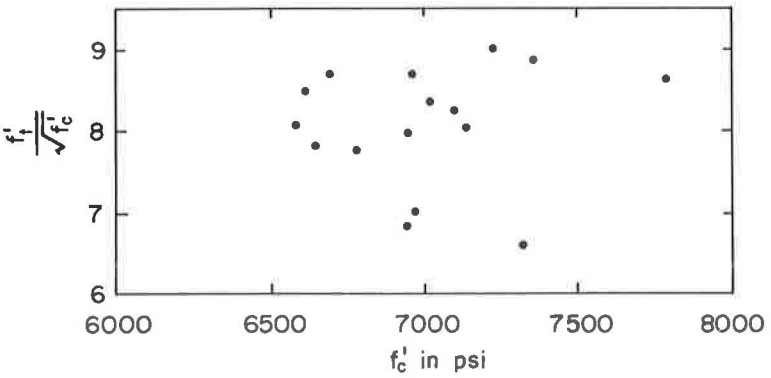

Figure 23. Variation in flexural tensile strength with compressive strength.

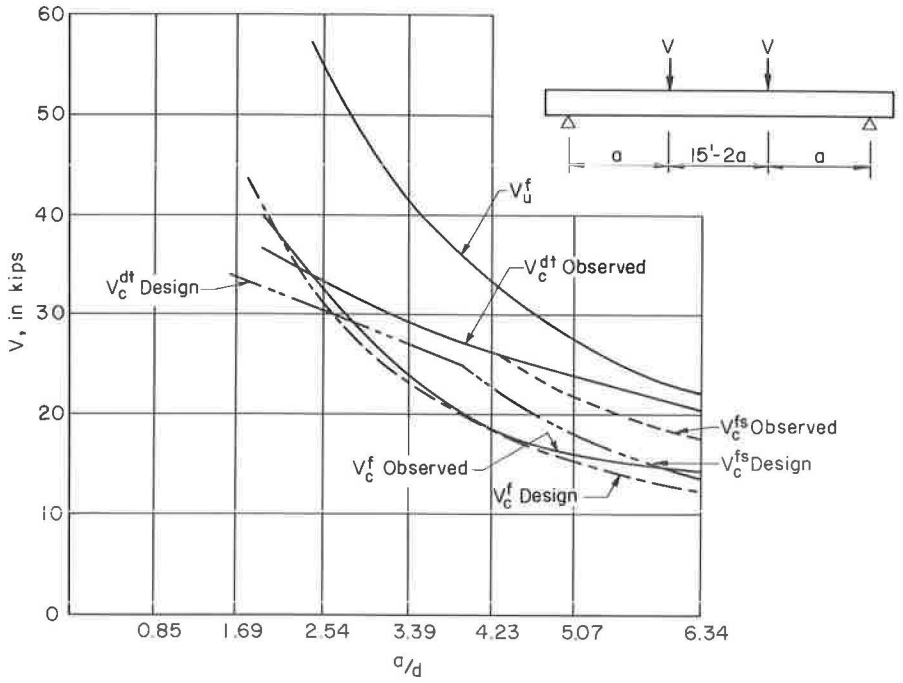

Figure 24. Comparison of observed and design strength of test beams.

of all test beams at inclined cracking (1), as shown for selected test beams in the Appendix, the critical principal tensile stresses at the intersection of the path of the diagonal tension cracks and the center of gravity of the cross-section, σ_t^{cg}, were estimated, and are recorded in Table 7. The average value of σ_t^{cg} determined in this manner was 430 psi, which corresponds to an average ratio of $\sigma_t^{cg}/\sqrt{f'_c}$ of 5.16. The minimum ratio of $\sigma_t^{cg}/\sqrt{f'_c}$ was 4.38, as determined for E.17. The recommendation of Hernandez, Sozen, and Siess was that diagonal tension inclined cracking should be considered to occur, for design purposes, when a principal tensile stress of $4\sqrt{f'_c}$ occurs at the intersection of the neutral axis with a 45° line drawn in the direction of decreasing moment from the extreme fiber in compression of the section considered. As may be noted from the figures in the Appendix, the values of the principal tensile

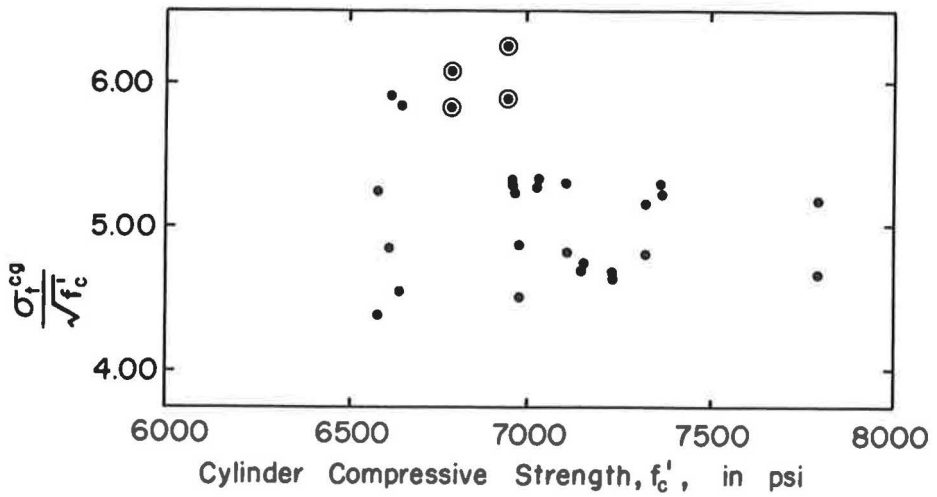

Figure 25. Relationship between principal tensile strength along cgc at diagonal tension cracking and compressive strength of concrete.

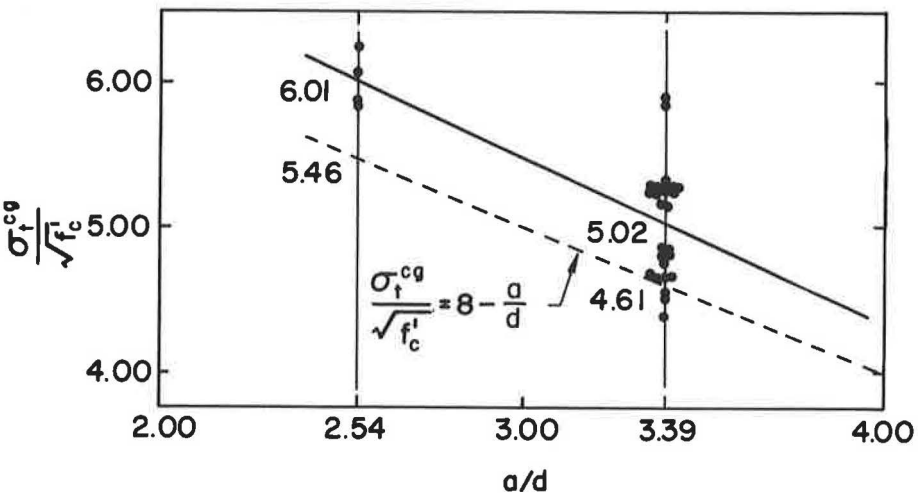

Figure 26. Relationship between tensile strength along cgc at diagonal tension cracking and a/d ratio.

stress along the neutral axis are relatively constant, because the dead load of the test beams is a small proportion of the total load at inclined cracking; therefore, the location of the section considered for diagonal tension cracking is not critical. Thus, it may be concluded that the recommendation of Hernandez, Sozen, and Siess would have conservatively predicted the diagonal tension inclined cracking of all of the test beams.

Values of $\sigma_t^{cg}/\sqrt{f'_c}$ are plotted against concrete strength in Figure 25 and the a/d ratio in Figure 26. In Figure 25, the four encircled points are for tests on an a/d ratio of 2.54; the remaining points are for tests on an a/d ratio of 3.39. Figure 25

indicates that, in the range of concrete strengths investigated, $\sigma_t^{cg}/\sqrt{f'_c}$ is relatively insensitive to changes in concrete strength. However, Figure 26 indicates that σ_t^{cg} varies with the a/d ratio. The following expression was selected for the principal tensile stress at the center of gravity causing diagonal tension cracking:

$$\sigma_t^{cg} = \left(8 - \frac{a}{d}\right)\sqrt{f'_c} \tag{14}$$

This expression has been plotted in Figure 26 for comparison with the test data. Based on Eq. 14, the applied load shear causing diagonal tension cracking may be calculated from the following equation, obtained from Eqs. 1, 2, and 3:

$$V_c^{dt} = \frac{Ib'}{Q^{cg}}\sqrt{\left(\sigma_t^{cg}\right)^2 + \left(\sigma_t^{cg}\right)\frac{F}{A}} - V_d \tag{15}$$

The V_c^{dt} design curve shown in Figure 24 was determined from Eq. 15 for an "average" test beam, assuming that V_d is equal to the dead load shear at the midpoint of the shear span. For a/d ratios of 2.54 and 3.39, V_c^{dt} is equal to 30.6 and 27.2 kips, respectively. Therefore, Eqs. 14 and 15 conservatively predicted all but two of the observed diagonal tension cracking shears on these a/d ratios. For the four observed diagonal tension cracking shears on an a/d ratio of 2.54, the average observed-to-predicted ratio was 1.09. For the 25 observed diagonal tension cracking shears on an a/d ratio of 3.39, the average observed-to-predicted ratio was 1.07.

Because $rf'_y/100$ is equal to $A_v f'_y/b's$, Eq. 7 may be written as:

$$\frac{rf'_y}{100} = \frac{V_u - V_c}{b'\beta d} \tag{16}$$

Flexural failures occurred in tests on a/d ratios of 2.54 and 3.39. Eq. 16 can be used to predict the least amount of web reinforcement required to develop the flexural capacity on these a/d ratios. The shear carried by the concrete, V_c, is assumed equal to the shear causing inclined cracking. For a/d ratios of 2.54 and 3.39, V_c^{dt} is less than V_c^{fs} and, therefore, V_c is equal to 30.6 and 27.2 kips, respectively. The applied load shear, V_u^f, required to develop the flexural capacity is 55.1 and 41.3 kips, respectively. Assuming that ℓ_e is equal to 11.5 in., β can be calculated from Eq. 8 after θ has been calculated using Eqs. 2, 3, and 4. β is equal to 1.38 and 1.46 for the a/d ratios of 2.54 and 3.39, respectively. Therefore, the amount of web reinforcement required to develop the flexural capacity of an "average" test beam on a/d ratios of 2.54 and 3.39 is $rf'_y/100$ equal to 417 and 226, respectively.

Four beams were tested on an a/d ratio of 3.39 with less web reinforcement than $rf'_y/100$ equal to 226. E.13 with $rf'_y/100$ equal to 222 and 162, failed in flexure, although it should be noted that the flexural capacity of E.16 was less than the other beams which failed in flexure. E.17 and E.18, with $rf'_y/100$ equal to 121 and 97, failed in shear.

Both beams tested on an a/d ratio of 2.54 had less web reinforcement than $rf'_y/100$ equal to 417. E.15, with $rf'_y/100$ equal to 222, failed in flexure. E.14 had the same amount of web reinforcement as E.15, except that the stirrups were not hooked in the tension flange. E.14 failed in shear because of inadequate anchorage of the stirrups below the inclined crack.

TABLE 8

BEAMS FAILING IN SHEAR

Beam	$\frac{rf'_y}{100}$ (psi)	$\frac{a}{d}$	V_c^{dt} (kips)	V_c^{fs} (kips)	V_c (kips)	V_u (kips)	Test / Predicted
E.1	0	6.34	14.4	13.8	13.8	13.8	1.48
E.2	0	5.07	20.0	18.0	18.0	18.0	1.33
E.3	0	4.23	23.5	22.9	22.9	22.9	1.13
E.4	0	3.39	27.2	31.8	27.2	27.2	1.10
E.17	121	3.39	26.8	32.0	26.8	34.4	1.10
E.18	97	3.39	27.0	32.0	27.0	33.1	1.17
E.14	222	2.54	30.8	51.6	30.8	40.1	1.34

Therefore, it can be concluded that Eq. 16 conservatively predicted the least amount of web reinforcement required to develop the flexural capacity of the test beams when loaded on a/d ratios of 2.54 and 3.39. Eq. 16 was more conservative for the lower a/d ratio, indicating that the closeness of the load point and the reaction had an influence on the amount of shear which was carried after diagonal tension cracking.

Eq. 16 can also be used to predict the shear strength of beams failing in shear. Solving for V_u:

$$V_u = V_c + b'\beta d \frac{rf'_y}{100} \tag{17}$$

The shear strength of the seven test beams which failed in shear was calculated from Eq. 17 and is given in Table 8. V_c^{dt} and V_c^{fs} were determined from Eqs. 13 and 15, respectively. V_c was assumed equal to the least value of V_c^{dt} and V_c^{fs}. Because the stirrups in E.14 were not hooked in the tension flange, ℓ_e was assumed equal to 8 in. The test-to-predicted ratios of shear strength ranged from 1.10 to 1.48; the average was 1.24. For the four beams without web reinforcement, the test to predicted ratios decreased from 1.48 to 1.10 as the a/d ratio decreased from 6.34 to 3.39, indicating that the prediction of the shear causing inclined cracking is more conservative for the higher a/d ratios. For the three beams with web reinforcement, the test-to-predicted ratios increased from 1.10 to 1.34 as the a/d ratio decreased from 3.39 to 2.54, indicating that the prediction of ultimate shear strength is more conservative for the lower a/d ratios.

CONCLUDING REMARKS

The following remarks are based on the tests on pretensioned I-beams reported herein and on the general discussion of overload behavior presented in this report. Concrete strengths of the tests reported herein varied between 6,500 and 7,800 psi.

1. Flexural cracking was observed at loads corresponding to computed tensile stresses in the extreme fiber in tension greater than that given by Eq. 12. The shear causing the development of significant inclined flexure shear cracking was greater than, although realistically predicted as, the shear expected to cause a flexural crack, based on Eq. 12, to form a distance from the concentrated load point in the direction of decreasing moment equal to the effective depth of the member.
2. The shear causing the development of inclined diagonal tension cracking in the tests reported herein was realistically predicted as the shear producing a principal tensile stress at the intersection of the path of the crack and the center of gravity given by Eq. 14.
3. Flexural failures occurred at strains in the extreme fiber in compression which varied between 0.0025 and 0.0028.
4. Of the seven test beams which failed in shear, five failed due to crushing of concrete in the web (four of which had no web reinforcement), one failed due to fracture of the web reinforcement, and the other failed due to inadequate anchorage of the web reinforcement in the tension flange.
5. The test results support the assumption that the ultimate shear which can be carried by the concrete above the top of an inclined crack is equal to the shear at inclined cracking.
6. The test results for a/d ratios of 2.54 and 3.39 indicated that the AASHO equation for design of web reinforcement:

$$A_v = \frac{1}{2} \frac{\left(V_u - V_c\right)s}{f'_y \, j \, d}$$

was conservative by a factor of roughly 3, with respect to a single cycle static load test.

7. An equation for the design of web reinforcement of the form of Eq. 7, in which β is determined from Eq. 8 for diagonal tension cracking or equals 1 for flexure shear cracking and V_c equals shear at inclined cracking, would have conservatively predicted the amount of web reinforcement required to prevent shear failures in the tests on an a/d ratio of 2.54 and 3.39 reported herein.

ACKNOWLEDGMENTS

This work has been carried out in the Department of Civil Engineering at Fritz Engineering Laboratory under the auspices of the Institute of Research of Lehigh University, as part of an investigation sponsored by the Pennsylvania Department of Highways, U. S. Bureau of Public Roads, and the Reinforced Concrete Research Council.

REFERENCES

1. Hanson, J. M., and Hulsbos, C. L. Overload Behavior of Prestressed Concrete Beams with Web Reinforcement. Fritz Engineering Laboratory Rept. No. 223.25, Lehigh Univ., Feb. 1963.
2. Hulsbos, C. L., and Van Horn, D. A. Strength in Shear of Prestressed Concrete I-Beams. Iowa State Univ., Engineering Experiment Station, Progress Rept. April 1960.
3. McClarnon, F. M., Wakabayashi, M., and Ekberg, C. E., Jr. Further Investigation into the Shear Strength of Prestressed Concrete Beams Without Web Reinforcement. Lehigh Univ., Fritz Engineering Laboratory Rept. No. 223.22, Jan. 1962.
4. Mattock, A. H., and Kaar, P. H. Precast-Prestressed Concrete Bridges 4. Shear Tests of Continuous Girders. Journal of the PCA Research and Development Laboratories, Vol. 3, No. 1, pp. 19-46, Jan. 1961.

Appendix

STATE OF CRACKING AT TIME OF INCLINED CRACKING

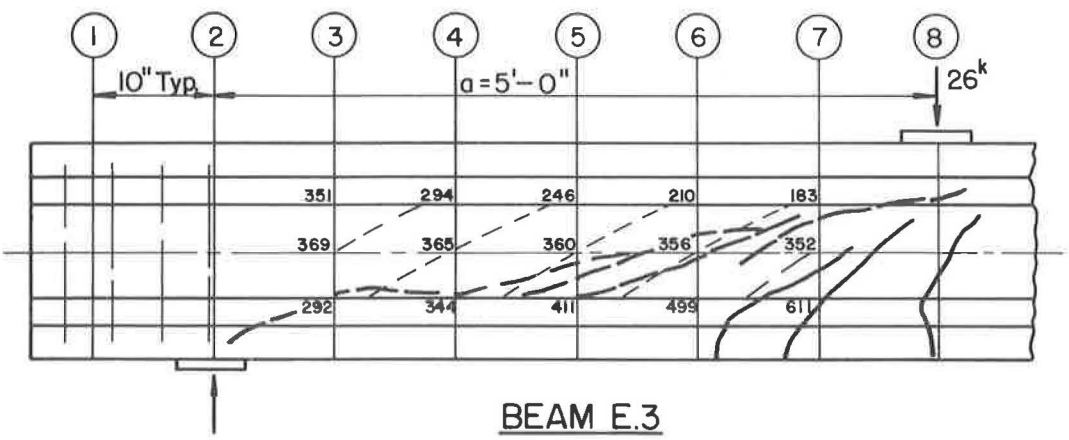

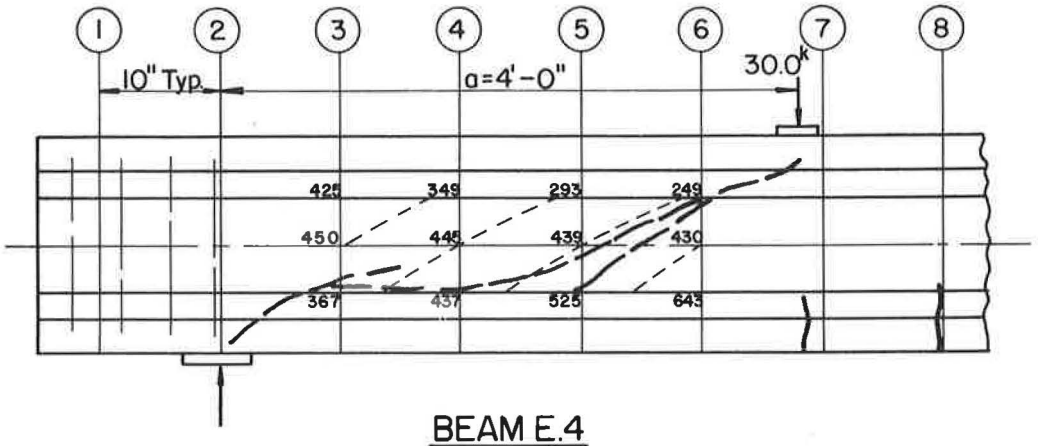

BEAM E.4

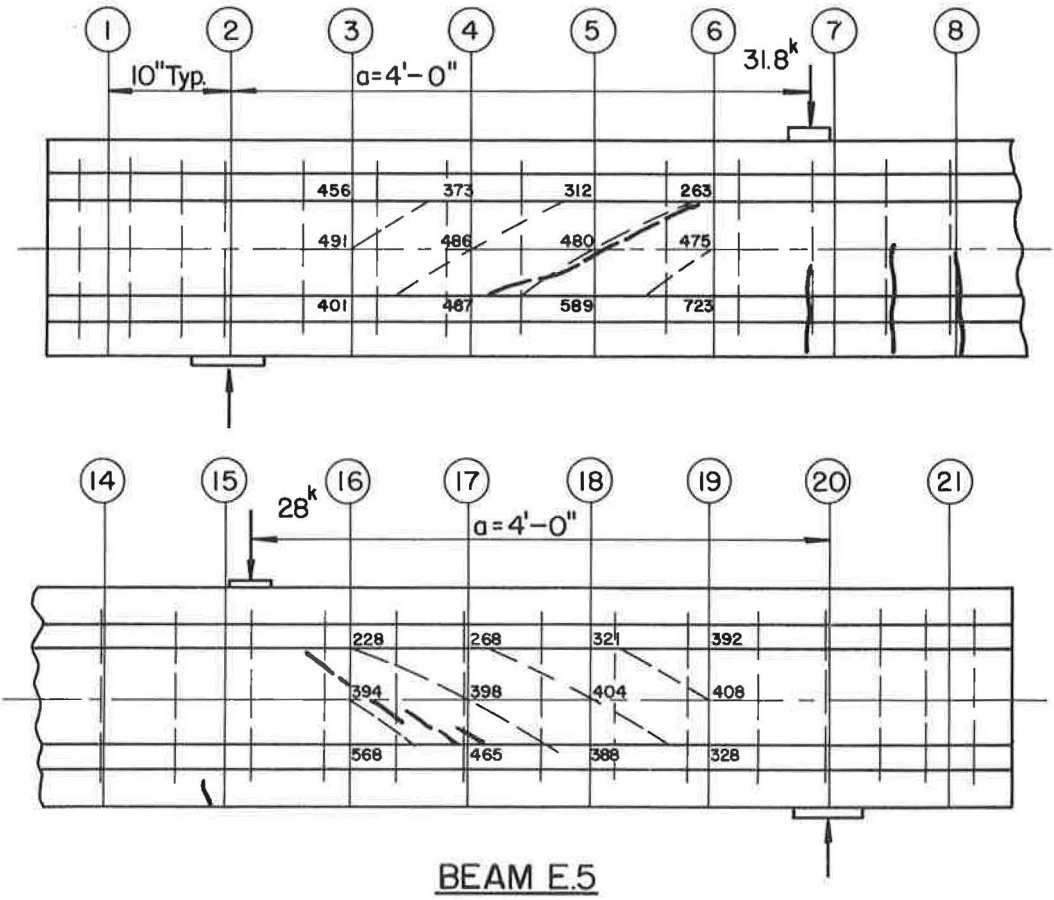

BEAM E.5

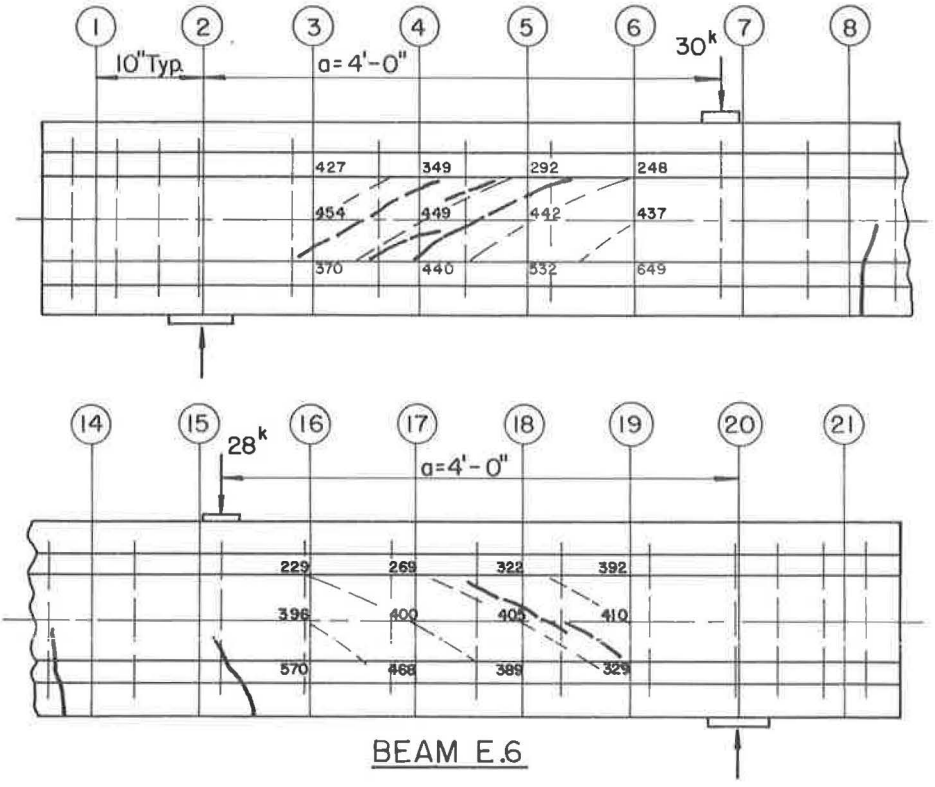

BEAM E.6

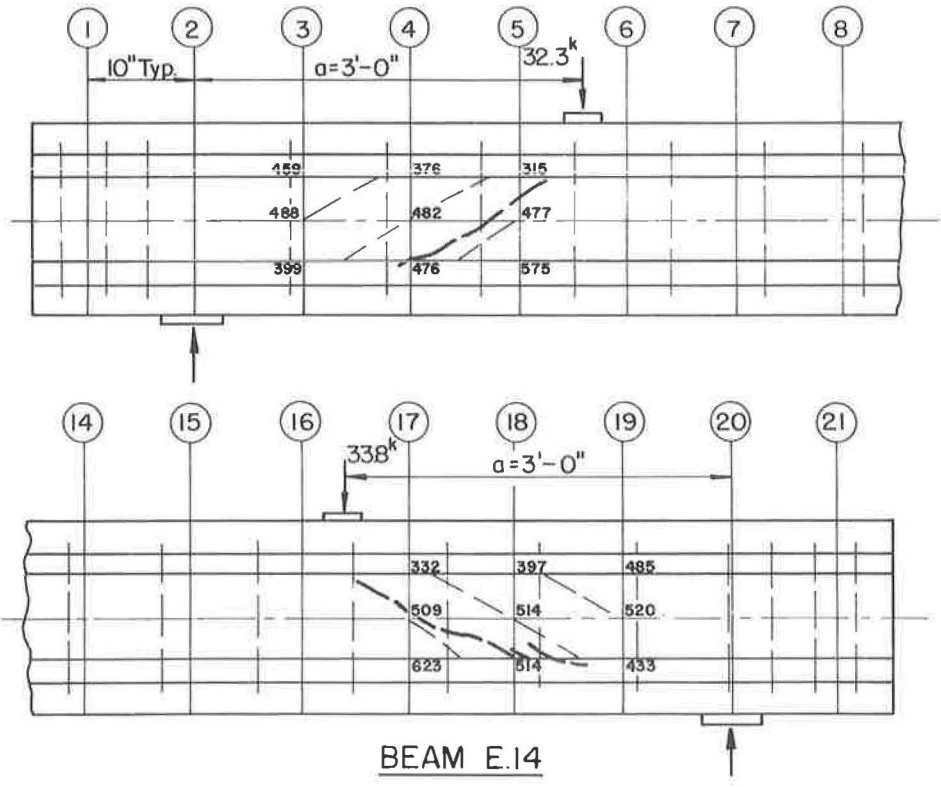

BEAM E.14

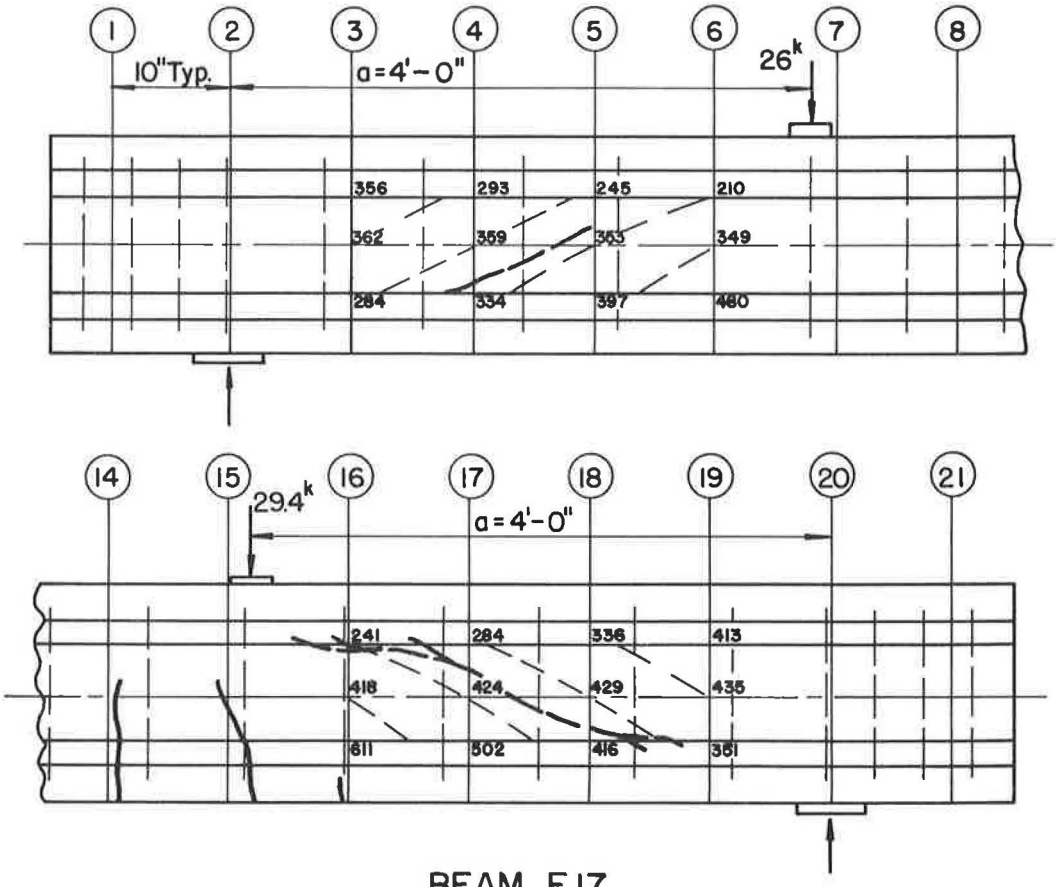
1
2
3
4
5
6
7
8
10"Typ.
a=4'-0"
26k
356
293
245
210
362
359
353
349
284
334
397
480
14
15
16
17
18
19
20
21
29.4k
a=4'-0"
241
284
336
413
418
424
429
435
611
502
416
361

BEAM E.17